Institut für Verfahrenstechnik,
Umwelttechnik und
Technische Biowissenschaften

DIPLOMARBEIT

Design Optimisation of a Bench-Scale Chemical-Looping Reactor by means of Flow Modelling

Ausgeführt zum Zwecke der Erlangung
des akademischen Grades eines Diplom-Ingenieurs

am Institut für

Verfahrenstechnik, Umwelttechnik und Technische Biowissenschaften
eingereicht an der Technischen Universität Wien
Fakultät für Maschinenwesen und Betriebswissenschaften

unter der Leitung von

Univ. Prof. Dipl.-Ing. Dr. Hermann HOFBAUER
Dipl.-Ing. Dr. Bernhard Kronberger
Dipl.-Ing. Dr. Tobias Pröll

von

Thomas Gurker
Viktorgasse 20/1/27
1040 Wien

Wien, im Jänner 2007   Thomas Gurker

Acknowledgements

First of all I would like to thank Prof. Dipl.-Ing. Dr. Hermann Hofbauer
for the opportunity to carry out this work at the Institute of Chemical Engineering.

In addition, I would like to express my sincere gratitude to Dipl.-Ing. Dr. Bernhard Kronberger
for his careful supervision of this thesis and for giving me excellent guidelines at the right
time. Moreover I would like to thank him for the creative input to this work and for his
numerous corrections.

I would also like to thank Dipl.-Ing. Dr. Tobias Pröll
for his continuous help and support and for reminding me to keep things simple.

A special thanks goes out to my colleagues for maintaining a warm and familiar atmosphere
and for their encouragement during the experimental work.

Finally, I would like to thank my family and friends for their patience
and constant moral support.

Kurzfassung

Unter den existierenden Technologien zur CO_2 Separierung und Speicherung (CSS) stellen Chemical-Looping Combustion (CLC) und Chemical-Looping Reforming (CLR) zwei neue und zukunftsweisende Technologien dar, die eine Abtrennung des Treibhausgases CO_2 zu vergleichsweise niedrigen Kosten ermöglichen.

In einem zirkulierenden Wirbelschichtsystem (CFB) bestehend aus zwei separaten Reaktoren, wird ein Metalloxid welches als Sauerstoffträger fungiert vom Luft Reaktor (AR) zum Brennstoff Reaktor (FR) transportiert. Dort wird das Metalloxid durch den zugeführten Brennstoff reduziert und zum AR zurücktransportiert, wo es durch den Luftsauerstoff reoxidiert wird. Der Hauptvorteil dieser Technologien liegt darin, dass das entstehende Rauchgas separat vom restlichen Abgas geführt wird, wodurch das CO_2 leichter abgetrennt werden kann.

Die vorliegende Arbeit repräsentiert die experimentelle Arbeit zur Weiterentwicklung eines kompakten Reaktorsystems im Labormaßstab für CLC und CLR. Basierend auf früheren Untersuchungen an einem existierenden Kaltmodell wurden verschiedene konstruktive Verbesserungen mit dem vorherrschenden Ziel der Reduktion der Gasleckagen durchgeführt. Dazu wurde das Strömungsverhalten des Feststoffes in zwei ähnlichen Reaktorkonzepten experimentell untersucht. Die Zirkulationsrate des Feststoffes und die Gasleckage wurden messtechnisch erfasst und gegenüber

- der Menge des eingesetzten Feststoffes

- des Volumenstromes im Luft Reaktor

- des Volumenstromes im Brennstoff Reaktor

variiert.

Zusätzlich wurden die Auswirkungen von geometrischen Veränderungen im Bereich des SLOTS und des DOWNCOMERS untersucht und die gemessenen Werte denen des Originalmodells gegenübergestellt.

Die durchgeführten Untersuchungen an dem leicht modifizierten Labormaßstabmodell mit einer Reaktorhöhe von 150 mm haben zu der Annahme geführt, dass Reibungseffekte, verursacht durch die Reaktorwände, sich auf die erhaltenen Messergebnisse auswirken. Dadurch konnten keine signifikanten Verringerungen der Gasleckage erzielt werden.

In Folge dessen wurde ein größeres Reaktormodell mit einer Höhe von 300 mm gebaut, und eine komplexere Annäherung an einen J-förmigen Siphon im DOWNCOMER-Bereich des Reaktorsystems implementiert. Auf diese Weise konnte die Gasleckage auf 0.5-4.5% des Brennstoff Reaktor Volumenstromes reduziert werden. Entsprechend konnte die Leckage auf 0.01-0.13% des Luft Reaktor Volumenstromes verringert werden. Die gefundenen Resultate belegen den Nutzen der Konzepte für die geplanten Anwendungen und es konnte ein Vorschlag für den Entwurf eines heiß betriebenen Laborreaktors erbracht werden. Schlussendlich wurde eine Zukunftsperspektive für die weitere Entwicklung und Anwendbarkeit des CFB Labormodells für CLC und CLR gegeben.

Abstract

Among several existing Carbon Capture and Storage (CCS) technologies, Chemical-Looping Combustion (CLC) and Chemical-Looping Reforming (CLR) are two new and promising technologies, capable to separate the greenhouse gas CO_2 at comparatively low costs.

In a circulating fluidised bed (CFB) system consisting of two separate reactors, an oxygen carrier in the form of a metal oxide is transported from the air reactor (AR) to the fuel reactor (FR). The metal oxide is reduced by the fuel and then transported to the AR where it is re-oxidised by the air. The main advantage of these technologies is that the combustion gas is kept separated from the rest of the flue gas, and so the CO_2 can be captured easily.

This thesis represents the experimental work carried out for the further development of a compact laboratory scale reactor system for CLC and CLR. Based on earlier investigations on an existing cold flow model, different design improvements with the predominating aim to reduce gas leakage between the two reactors were carried out and the fluid dynamics of two similar reactor concepts were studied experimentally. The solid circulation rate and the gas leakage were investigated against variation of

- amount of solid inventory

- fluidisation rate of the air reactor

- fluidisation rate of the fuel reactor

Additionally, the effects of geometrical modifications of the downcomer and the slot section were studied and the measured values were compared with the original model.

Investigations on the slightly modified small scale cold flow model with a reactor height of 150mm, led to the assumption that friction effects caused by the reactor walls have strong influence on the measurements, as design improvements could not significantly lower the gas leakage between the reactors.

As a consequence a larger reactor flow model with a reactor height of 300 mm was built and a complex approach to a J-type loop seal was implemented in the downcomer section of the reactor. It was found that the gas leakage could be minimised to 0.5-4.5% of the fuel reactor inlet gas stream. Accordingly, the leakage was minimised to 0.01-0.13% of the air reactor gas stream. The findings of the experiments show the suitability of the concepts for the planned applications and a design proposal for a hot laboratory unit is given. Finally, a future

outlook about the further development of small scale CFB reactor systems for CLC and CLR is given.

The punishment of Prometheus for giving fire to mankind (T. Velasquez).

Table of Contents

1 Introduction

1.1 Worlds Energy Demands and Greenhouse Gas Problem

It is generally accepted that greenhouse gases contribute to an increased global average temperature on earth. During the last century a significant rise in the concentration of carbon dioxide in the atmosphere was measured, whereby the main part of the anthropogenic release comes from combustion of fossil fuels. If governmental policies will not be changed in the future, the world primary energy demand will rise by 60% from 10.3 billion tonnes of oil equivalent (btoe) in 2002 to 16.5 btoe in 2030, whereby two thirds of the increase will come from developing countries. In this period of time, fossil fuels are expected to account for almost 90% of the worldwide growth in energy demand. Oil will remain the single largest fuel in the global primary energy mix, although its share will fall marginally. The demand for gas will expand faster than the demand for any other fossil fuel by 2030 and gas will have overtaken coal as the world's second largest energy source [2].

Oil & Gas Journal [3] estimates that the worldwide reserves were 175.4 million tonnes of oil (OPEC 122.5) and 173 billion m^3 of natural gas (OPEC 89.2) in the year 2005. This represents another 50 years of remaining reserves of oil and over 65 years of natural gas. Interestingly, that theory has been around since the 1970s and in fact, the figures for years of remaining reserves have remained relatively constant over the past few decades. Industry has replaced consumption with newly discovered oil and gas deposits and has developed technologies to increase the amount of oil and gas that can be recovered from existing reservoirs like Enhanced Oil Recovery (EOR) or Enhanced Gas Recovery (EGR).

However, estimates of the Oil and Gas Journal for worldwide oil reserves are 1.2% higher than the prior year, not taking into account the above mentioned improving production technologies [3].

The projected increase in world energy demand is expected to drive CO_2 emissions up to 62% between now and 2030 and power generation is estimated to contribute roughly half of the total expected increase in the global greenhouse gas emissions. In the following figures a comparison between global and EU energy-related CO_2-emissions is shown. Figure 1-1 demonstrates that since 1970 CO_2-emissions within the EU region have almost stabilised, whereas on the contrary, a continuous rise in the global emissions is predicted according to Figure 1-2.

Firstly, this demonstrates that efforts have been undertaken in the past to lower CO_2 emissions, but, secondly, it should be mentioned that 46% of electricity production in the European Union is already carbon-free, because it comes from nuclear or renewable energy sources. The fact that in the western EU countries huge efforts to minimise costs for power generation by improving energy efficiency have been undertaken also contributes to the stabilised CO_2 emissions [2].

Probably even more influential on the CO_2-emissions within the EU region was the political and economical breakdown in countries of the former eastern block. Industrial production without pursuing environmental policies would have led to a different scenario today.
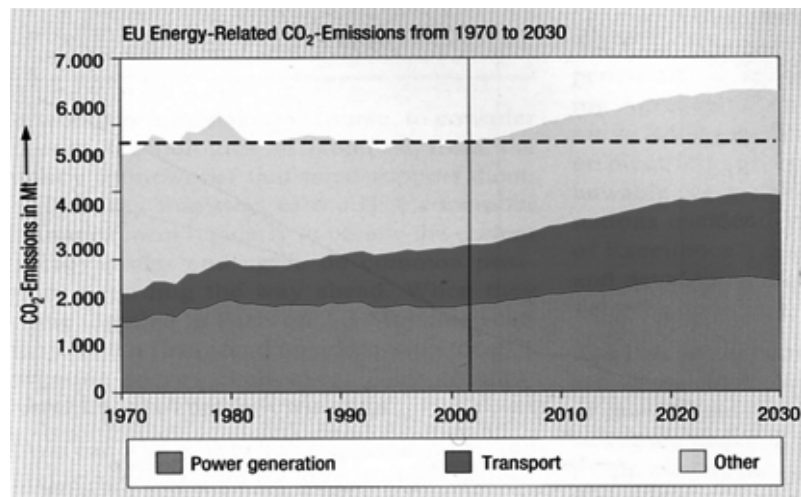

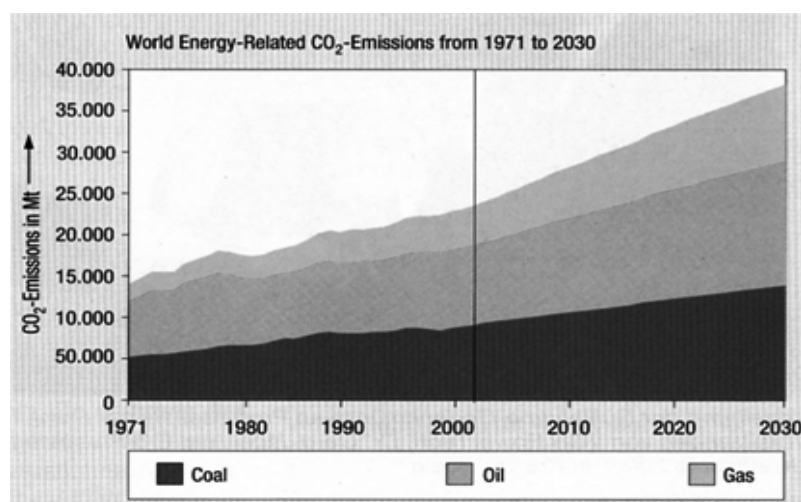**Figure 1-1: EU CO_2 emissions from 1970 to 2030 [2]**

Figure 1-2: Global CO_2 emissions from 1971 to 2030 [2]

According to the Kyoto Protocol, the European Union has adopted a directive [4] in which the Council underlined the urgent need for concrete action on Community level. The Programme recognises that the Community is committed to achieving an 8% reduction in emissions of greenhouse gases by 2008 to 2012 compared to 1990 levels, and that, in the longer-term, global emissions of greenhouse gases will need to be reduced by approximately 70% compared to 1990 levels.

In a business-as-usual scenario, however, the EU will still not reach its Kyoto target and more rigorous policies seem to be compulsory. The International Energy Agency (IEA)
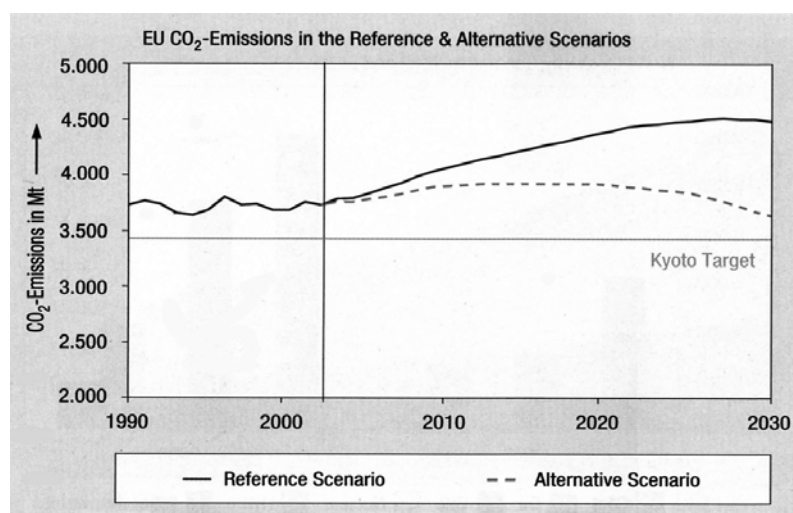

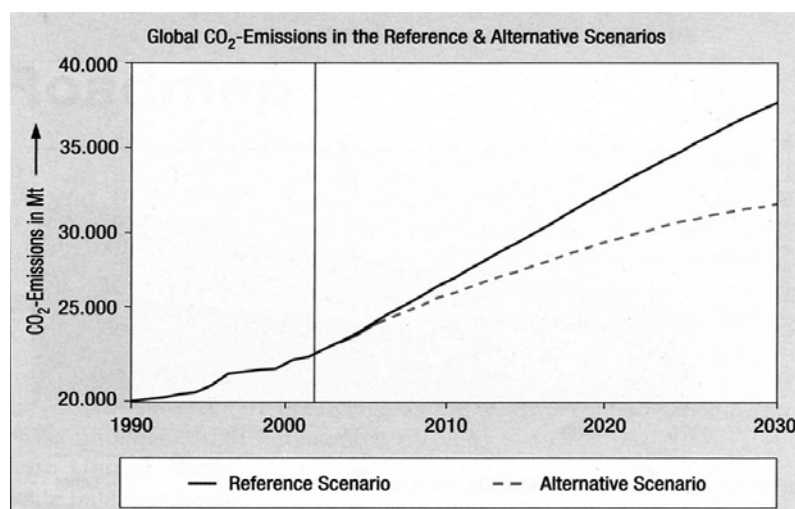**Figure 1-3: EU CO$_2$ emissions in the reference and alternative scenarios [2]**

Figure 1-4: Global emissions in the reference and alternative scenarios [2]

modelled a World Energy Outlook's Alternative Scenario [5], which considers measures like improved energy efficiency, more electricity from combined heat and power, supported renewables, and faster deployment of advanced technologies in developing countries. Figure 1-3 shows that this scenario could stabilise the EU CO_2-emissions by 2010 and decline after 2020. The alternative scenario's 16% reduction of global CO_2-emissions by 2030 may look impressive (Figure 1-4) but this improvement is still far from the reduction necessary to stabilise greenhouse gas concentration in the atmosphere.

To achieve further reductions in CO_2 emissions substantial measures need to be realised quickly. Renewable energy sources need to be constituted on top of the list in the policy framework within the next years. However, the potential of substitution of fossil energy at moderate costs clearly is limited and a variety of technology options are going to play a major role in the future. So-called Zero-Emissions Technologies (ZET) for fossil fuels have become a broadly accepted option to renewable energy and nuclear power solutions.

1.2 CO_2 Sequestration for Fossil Fuel Power Plants

On first sight, putting CO_2 back to earth does not seem to be technically sophisticated, but a recent IEA modelling suggests that CO_2 capture and storage (CCS) technologies are expected to play a significant role in the future, so long as CO_2 is priced at 10 USD to 20 USD per tonne, or more [2]. This, however, is what is generally meant by the term CO_2 sequestration and among several concepts, Geological Storage (GS) and the closely related Enhanced Oil and Gas Recovery (EOR/EGR) are established as serious and save technologies.

The process of geological storage means that the injected greenhouse gas either remains trapped and sealed in the reservoir or it may react chemically with the reservoir rocks and fluids to become part of the reservoir itself. The main storing options are ageing and depleted oil and gas reservoirs, deep saline reservoirs and unmineable coal seams (Figure 1-5). In the case of oil and gas reservoirs, CO_2 is essentially returned to formations that already contain hydrocarbons and many of these formations have retained oil, gas or water in isolation from surrounding rocks for millions of years.

After more than a century of intensive petroleum exploration, thousands of oil and gas fields are approaching the ends of their economically productive lifes. CO_2 can be used in the EOR-process to recover more oil. In most oil fields only a portion of the original oil in place is recovered using standard petroleum extraction methods. EOR used as a secondary oil

recovery technique has the potential to increase an oil field's ultimate recovery of oil up to 60% and extend the oilfield's life by decades.
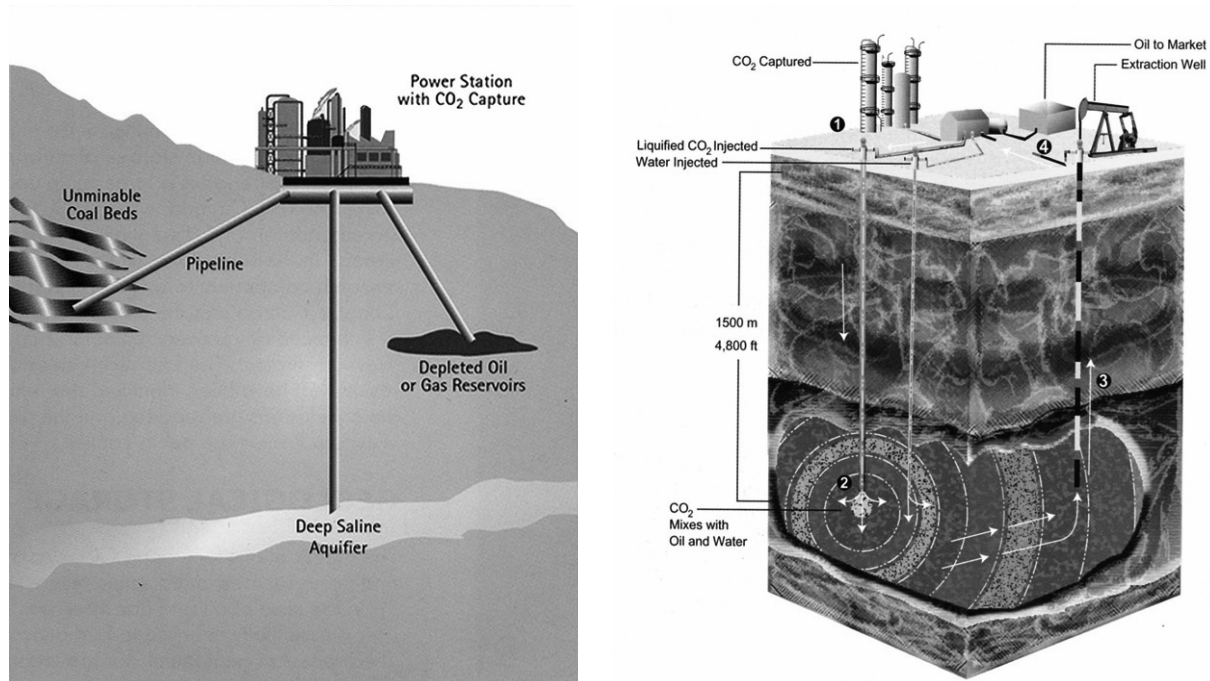

Figure 1-5: Carbon capture and storage (CSS) technologies [7]

When the CO_2 is injected for EOR, it contacts oil that cannot be produced conventionally and causes it to swell and become less viscous. If the subsurface rock is thought of as sponge with pores containing the oil, then the swelling of the oil helps to push a portion of the oil out of the pores. The reduced viscosity then improves the flow of oil to the production wells. This technique is well established and a lot of research work has especially been done on this topic [6]. If additionally, the CO_2 is stored in the oil reservoir, value is added to the process, and EOR is an environmentally as well as an economically attractive option [7].

According to Gielen and Podkanski [8] the main application of CCS is for electricity production. There are also certain opportunities in manufacturing industry and in fuel processing, whereas a promising strategy could be a cogeneration of electricity and synfuels from coal with CO_2 capture. Compared to a process without capture, CCS will always increase production costs, and the main task now is to develop low cost capture technologies with a small energy penalty.

1.3 Chemical-Looping Technologies

In terms of energy technologies "Chemical-Looping Technologies" describe two distinct processes that have in common that a species is chemically bound on a solid phase in one reactor and released in a second one, which leads to cyclical reaction and regeneration. As a more energy-efficient combustion method, Salvador, C. et al [9] investigated the carbonation-calcination reaction of CaO in a FBC environment, as a potential method for CO_2 capture from flue gases at high temperatures.

In this work, however, by chemical-looping processes are meant that oxygen is transferred by means of metal oxides from air to the fuel with no direct contact between fuel and air. Thus, the reactor system consists of two connected fluidised beds that exchange solids but not gases, which can basically be described as circulating fluidised bed (CFB) systems. These facts make an inherent separation of the flue gases possible, which is important if CO_2 separation is considered or if the flue gas from one of the reactors is the desired product. In an industrial scale application, the released heat of the system can be used for power generation.

1.3.1 Chemical-Looping Combustion

The key advantage of Chemical-Looping Combustion is that additional costs can be kept significantly lower compared to other CCS technologies. It is based on an inherent CO_2 separation technology, which reduces the technical effort of the sequestration to pressurisation and transport of the CO_2.

CLC was first mentioned by Richter and Knoche [10] and involves the combustion of fuel, using a metal oxide as an oxidant instead of oxygen from ambient air. The main advantage of this technology, in view of the CCS technologies, is that the combustion gas is kept separated from the rest of the flue gas, and so the CO_2 can be captured easily.

The system consists of an air reactor (AR) and a fuel reactor (FR) and an oxygen carrier in the form of a metal oxide that transports oxygen from the air to the fuel (Figure 1-6). In the FR, the metal oxide is reduced by the fuel and then transported to the AR where it is re-oxidised by the air. The outlet gas from the air reactor (flue gas) consists mainly of N_2 and some non-reacted oxygen, while the outlet gas of the fuel reactor (combustion gas) consists of CO_2 and water.
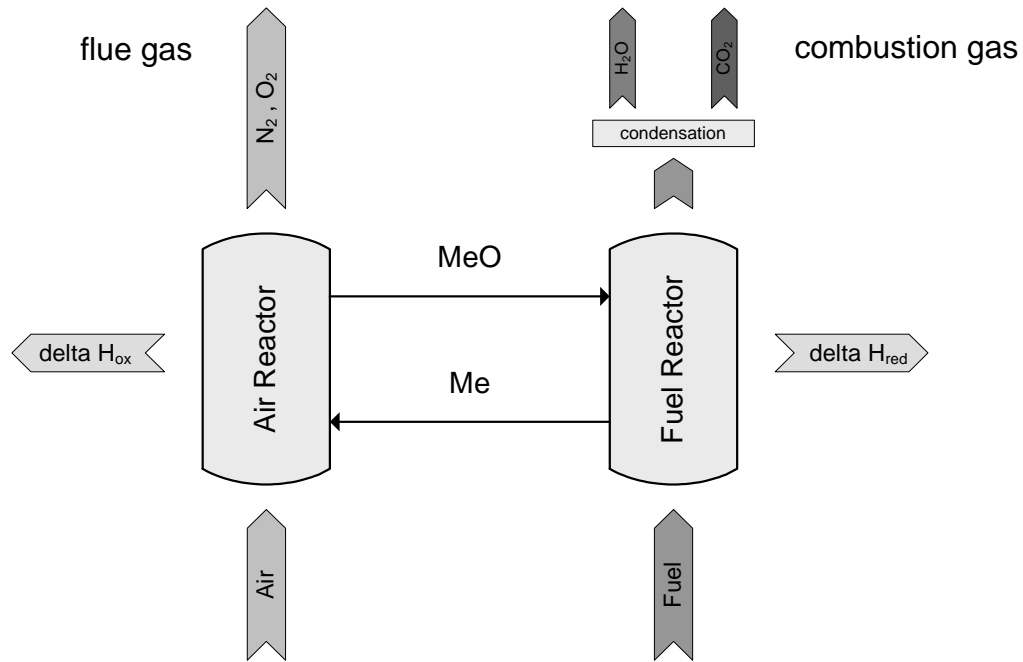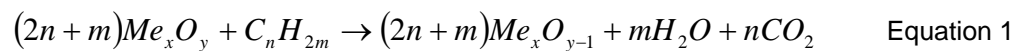
**Figure 1-6: Principle of chemical looping combustion. MeO and Me denote oxidised and reduced oxygen carriers**

In the fuel reactor, the oxygen-carrier reacts with the gaseous fuel, according to:

$$(2n+m)Me_xO_y + C_nH_{2m} \rightarrow (2n+m)Me_xO_{y-1} + mH_2O + nCO_2 \qquad \text{Equation 1}$$

The reduced oxygen carrier is transported to the air reactor where it is oxidized by the incoming air, according to:

$$Me_xO_{y-1} + \frac{1}{2}O_2 \rightarrow Me_xO_y \qquad \text{Equation 2}$$

The total reaction is the sum of reactions in Equation 1 and Equation 2 and is the same like for conventional hydrocarbon combustion with air:

$$C_nH_{2m} + \left(n + \frac{m}{2}\right)O_2 \rightarrow mH_2O + nCO_2 \qquad \text{Equation 3}$$
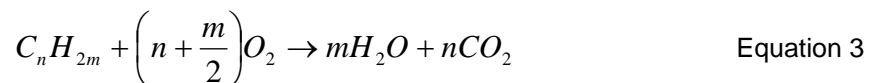
Reaction in Equation 1 is mostly endothermic and reaction in Equation 2 is always exothermic, depending on the type of metal oxide used in the process. Also, the amount of net heat released in the process is equal to normal combustion, according to:

$$\Delta H_c = \Delta H_{ox} + \Delta H_{red} \qquad \text{Equation 4}$$

Due to this fact, the oxidisation reaction (Equation 2) must have a higher heat of reaction, than the conventional combustion reaction, which means more heat is released at a high temperature through recovery of thermal energy at a low temperature in the fuel reactor. This "chemical heat pump" effect can increase the overall thermal efficiency of the power
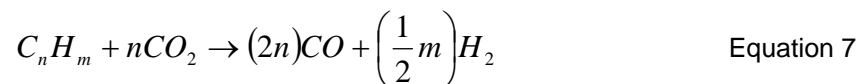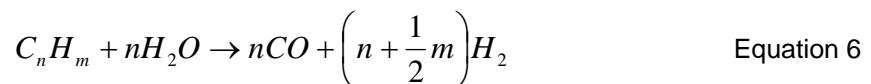
generating system as reported by Anheden, M. et al [11] and, originally, by Richter and Knoche [10]

1.3.2 Chemical-Looping Reforming

Another application of the chemical looping technology is its potential in reforming reactions to produce synthesis gas. Rydén et al [12] investigated the reforming of natural gas for hydrogen production with carbon dioxide capture and named the process chemical looping reforming. The overall reaction can be described as partial oxidation (Equation 5) because of an under-stoichiometric oxygen supply. Again, the exothermic reaction takes place in the air reactor according to Equation 2.

$$C_nH_m + \left(\frac{1}{2}n\right)O_2 \rightarrow nCO + \left(\frac{1}{2}m\right)H_2 \qquad \text{Equation 5}$$
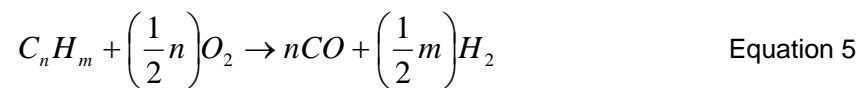
In the fuel reactor, beside partial oxidation, also complete oxidation (Equation 1), steam reforming (Equation 6) and CO_2 reforming (Equation 7) take place. If steam or CO_2 is added to the process the relative importance of those reactions could be enhanced, which would consequently lead to an increased production of the yielded synthesis gas.

$$C_nH_m + nH_2O \rightarrow nCO + \left(n + \frac{1}{2}m\right)H_2 \qquad \text{Equation 6}$$

$$C_nH_m + nCO_2 \rightarrow (2n)CO + \left(\frac{1}{2}m\right)H_2 \qquad \text{Equation 7}$$

However, steam reforming, CO_2 reforming and complete oxidation should not be allowed to dominate the process since that would make the overall process endothermic and external heating would be necessary. With proper settings of the chemical looping reforming system, the reformed gas is a mixture of H_2, CO, H_2O and CO_2. This can be used as a feedstock for the production of pure H_2 through a following water-gas shift reaction or for the production of hydrocarbon fuels in a Fischer-Tropsch process.

Summed up, it can be seen that CLC and CLR are two related technologies that can preferably be built in a CFB system. One additional advantage of this fact is that both technologies could be realised in basically the same reactor system without extensive adoptions of the construction.

2 Scope and Outline

Due to the constant circulation of the metal oxide in Chemical-Looping Technology (CLC or CLR) reactor systems, certain amounts of gas are transferred through the orifices that interconnect the two reactors. The gas leakage into the air reactor produces a loss in the CO_2 capture efficiency, whereas the leakage into the fuel reactor dilutes the CO_2 flow at the exit of the fuel reactor. Both effects need to be minimised when an industry scale application of this new technology is considered.

In this thesis, two laboratory scale cold flow models for CLC are investigated with the predominating aim to minimise gas leakage between the two reactors by a variation of design properties.

In the first part of this work some improvement opportunities in the critical parts of an existing cold flow model should be implemented and lead to a better understanding of the circulating fluidised bed system. The basic layout of the rector, which was originally designed by Kronberger et al. [13] as a cold flow model and later transferred into a hot laboratory unit by Johansson et al. [14], is shown in the following chapter. The basic idea in this comparably small reactor design was to reduce the complexity of the process.

In the second part of this work the attained knowledge of the small laboratory unit should be applied in a newly constructed reactor design at a slightly larger scale. Main arguments for the increase in scale were the significant wall effects detected during the work with the small-scale unit. Although it is clear that the transfer (scaling) of the results for the hot unit will not follow the fluid dynamic similarity any more, a number of arguments support this approach.

Investigations upon the behaviour of different operation conditions of the reactor should be conducted. Therefore, the amount of solid inventory and the fluidisation rates in the reactors are varied. Also, the influence of certain design variations like modification of the orifice geometry on gas leakage and solid circulation rate are measured and compared with the original design of the reactor.

Finally, the findings of this study should serve as design recommendations for the modification of the existing "hot" reactor unit [14] for CLR operation.

3 Existing Reactor Designs of Small Scale Circulating Fluidised Bed Reactors

A lot of designs for internally circulating fluidised bed reactors have been proposed for various processes. In the following chapter a short overview is given, whereby the main focus of the considerations is given to the potential to avoid gas leakage between the reactors and on a compact design with short transport lines for the circulating solids. To compare the different concepts some of the designs are depicted and described in detail, by presenting a diagram along with the characteristic design properties. Additionally, the rates of

- solid circulation / solid inventory

- gas leakage / inlet volume flow

- gas leakage / solid circulation

were calculated and, where possible, an assessment of the applicability of the particular design to a small CLR reactor unit is given.

3.1 Adjacent Compartment Reactors

Chong et al. [15] introduced a reactor system, in which two adjacent cubical reactors are interconnected via two openings to permit the movement of solids in both directions, but to provide an effective seal against gas mixing. The adjacent configuration has the advantage that the system is very compact and that the two reactors are separated by a centre reactor wall, which allows heat transfer. Consequently, the transport lines for the solids are short and can be realised without any moving parts. The reactor system was originally patented as an oil shale retort for the gasification of oil shale and the combustion of the residual carbon. The upper orifice is designed as a chute where the particles flow in the form of a packed bed into the other chamber. It was found that a triangular deflector plate, fixed above the lower orifice, deflects gas away from the chute and discourages leakage from right to left. With a cross section of the retort of approximately 150mm x 150mm, a maximum throughput of about 4.2 g/s could be achieved. The unit operated in the steady state for sustained periods without provision for controlling the solids circulation rate.

Reichhold et al. [16] used the principle for a continuous adsorption and desorption process to separate and recover gaseous pollutants and reusable compounds in a similar apparatus (Figure 3-1). The cross section of each reactor was 221mm x 225mm with a height of

490mm. The horizontal openings in the dividing reactor wall had a height of 35 mm and as the two beds were fluidised at different rates (V1<V2), the bed material started to circulate.
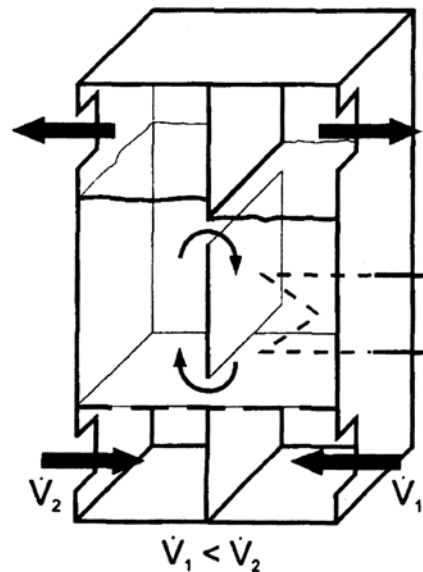

Figure 3-1: Internally circulating fluidised bed acting as a reaction and regeneration system [16].

Fang et al. [17] made investigations on solid circulation rate and gas leakage using a two dimensional test facility with two orifices allocated on an internal divided wall with the possibility to adjust the height and distance of the orifices. With an overall height of 2m and a cross section of 280mm x 40mm of each reactor the effects of bed material, gas velocities and orifice allocation and size were investigated and the effects on gas leakage and solid circulation demonstrated.

Snieders et al. [18] used a small four compartmented interconnected fluidized bed to investigate the potential for the combustion of biomass and the behaviour of cylindrical pellets in a bed material of glass ballotini. The reactor with a cross section of 190mm x 190mm was subdivided into four rectangular, separately fluidised compartments. The material flows upwards in the two fast beds, is then thrown over a weir into the corresponding slow bed where it flows downwards and enters the following fast bed through an orifice in the separating wall. The distribution of pellets over the compartments after a given fluidisation time, the pellet circulation time and the dynamics of one radio-active pellet was measured by the use of the so called Positron Emission Particle Tracking technology.

Detailed research on the four compartmented reactor system has also been done by Korbee, R. [19] and Snip, O.C. [20] using an interconnected fluidised bed (IFB) for regenerative desulfurisation of coal. In this process, combustion and sulphur capture are integrated with sorbent regeneration into one reactor system. Figure 3-2 shows the principal setup of the reactor system consisting of a combustor for sulphur capture (1), transporting the ash and sorbent over a weir to a compartment with solids downflow (2) and segregation of ash and sorbent.
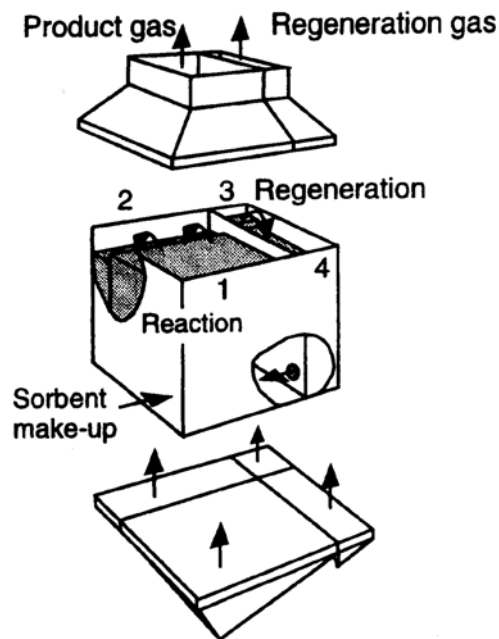

Figure 3-2: Schematic presentation of an IFB reactor suitable for solids circulation in a reaction-regeneration process [20].

From this compartment the solids are transported to a regenerator (3) where the sorbent is regenerated by means of reducing gases and finally transported over a weir to a de-fluidised compartment (gas velocity below the minimum fluidisation velocity), which was used to control the circulation rate by means of adjusting the gas velocity.The reactor had a cross section of 200mm x 200mm, with a significantly smaller constructed regenerator (60mm x 60mm) because the regeneration of the sorbent is fast compared to the sulphur capture process.

Kronberger et al. [13] and Johansson et al. [14] used a two compartment reactor as a cold flow model for Chemical-Looping Combustion (Figure 3-3). The reactor consisted of two interconnected reactors with a centrally located chute, acting as a downcomer for the

fluidised particles. After being transported over a weir, due to the stronger fluidisation in the air reactor, the particles formed a packed bed in the downcomer. The particles travelled downwards as a solid column that acted as a gas lock and then fell into the fuel reactor. A small slot in the partition wall, located at the bottom area of the reactor, acted as a return orifice that transported the particles back to the air reactor and closed the circle. As already mentioned above, the system represented a very compact and good implementation of a complex CFB reactor system.
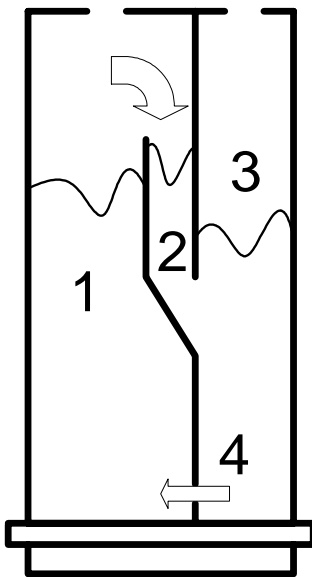

Dimension air reactor	0.019x0.027	[m]
Dimension fuel reactor	0.019x0.019	[m]
Height of reactor	0.12	[m]
Particle diameter	70	[μm]
Particle density	1500	[kg/m^3]
Total solid inventory	0.053	[kg]
Air reactor gas velocity	1.9	[u_t]
Fuel reactor gas velocity	21	[u_{mf}]
Slot height	0.0012	[m]
Solids circulation rate	0.00044	[kg/s]
Minimum fluidisation velocity	0.00237	[m/s]
Rate: Solid Circ / Solid Inventory	0.0083	[1/s]
Rate: Gas Leakage / Gas Inlet	0.0185	[-]
Rate: Gas Leakage / Solid Circ Rate	0.0049	[m^3/kg]

Figure 3-3: Two compartment reactor; 1 … air reactor, 2 ... downcomer, 3 … fuel reactor, 4 … slot

Table 3-1: Characteristic design properties of two compartment reactor

3.2 Rotating Cone Reactor

Wagenaar, et al. [21] proposed a novel interconnected fluidised bed for the combined flash pyrolysis of biomass and combustion of the produced char. To obviate the disadvantages like the large carrier gas stream, extra heating and a large downstream equipment of conventional circulating fluidised beds, a reactor type which enables high solids throughput without requiring any transport gas was developed. The heart of this reactor consists of a rotating cone, in which biomass particles are mixed intensively with an excess of hot sand particles. The circulating hot sand provides the heat for the pyrolysis process and prevents fouling of the cone wall. Janse, et al. [22] proposed an advanced version of the reactor (Figure 3-4) where the rotating cone is partly submerged in a fluidised bed and sand flows through supply openings near the bottom of this cone. Due to centrifugal forces, sand particles flow along the cone wall in upward direction, pass the upper edge and fall back into

the fluidised bed (internal circulation loop). To combine the pyrolysis reactor with a section for char combustion, both, char and sand are now transported through an orifice to the combustor. There the sand is reheated before being recycled to the pyrolysis reactor by means of a standpipe, riser and cyclone.

The gas flow through the orifice between the pyrolysis reactor (reductive atmosphere) and the combustor (oxidative atmosphere) is studied because this gas flow must be minimised to avoid the formation of explosive gas mixtures or a significant loss of the bio-oil vapours. It was found that the leakage gas flow from the pyrolysis reactor to the combustor was approximately 2% of the pyrolysis reactor inlet gas flow. However, the gas flow from the combustor to the pyrolysis reactor could not be detected by the experimental procedure. In Table 3-2 the characteristic parameters of the experimental setup are shown:
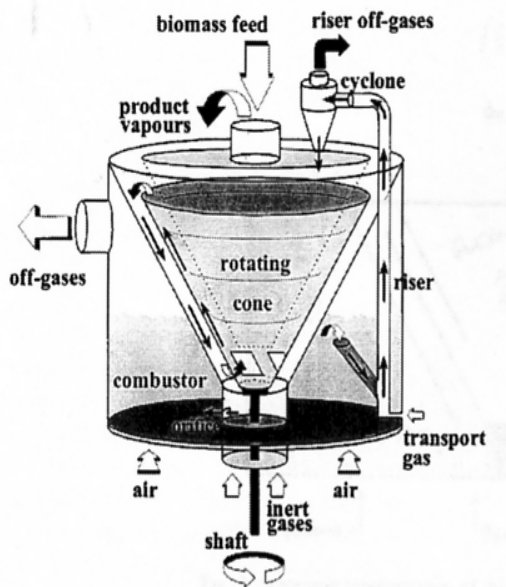

Figure 3-4: Rotating cone reactor [22]

Diameter rotating Cone reactor	0.39	[m]
Height rotating cone reactor	0.40	[m]
Half cone top angle	30	[°]
Particle diameter	390	[µm]
Particle density	2605	[kg/m^3]
Total solid inventory	25	[kg]
Minimum fluidisation velocity	0.08	[m/s]
Combustor gas velocity	1.78	[u_{mf}]
Orifice diameter	0.02	[m]
Solids circulation rate	0.025	[kg/s]
Pyrolysis reactor gas velocity	1.37	[u_{mf}]
Rate: Solid Circ / Solid Inventory	0.001	[1/s]
Rate: Gas Leakage / Gas Inlet	0.0252	[-]
Rate: Gas Leakage / Solid Circ Rate	0.0022	[m^3/kg]

Table 3-2: Characteristic design properties of rotating cone reactor

3.3 V-valve Reactor

The V-valve belongs to the class of non-mechanical valves which includes the L-valve and the J-valve. Li et al [23], Liu et al [24] and Leung et al [25] investigated the behaviour of a V - valve, connected to an overflow standpipe and found some unusual but important characteristics like cyclic operation at low solid flow and hysteresis effects due to certain design specifications. Guigon et al [26] achieved some interesting results regarding the flow controllability of the solids, focusing on different geometries of V-valves.

Bhattacharya, et al. [27] investigated the solid circulation behaviour in a compartmented fluidised bed using a pair of V-valve and riser combination (Figure 3-5). The reactor has an overall height of 500 mm and is divided in the ratio 2:1 by a partition plate with two orifices at the height of 130 mm and 240 mm, respectively. The V-valve (V) collects the fluidised sand like a hopper and transports it through the orifice into the riser (R), where it falls over a weir into the other part of the reactor. The effects of bed aeration, V-valve aeration, riser aeration and particle size were investigated by numerous measurements, whereas air velocity through the bed, V-valve and riser was varied in the range of 1-4 u_{mf}, 5-60 u_{mf} and 0-65 u_{mf}.
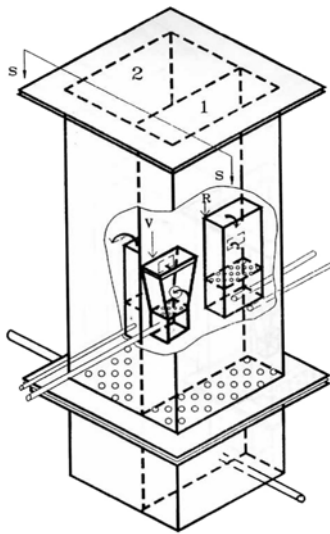

Figure 3-5: V-valve reactor [27]

Reactor width	0.24	[m]
Reactor depth	0.24	[m]
Reactor height	0.5	[m]
Average particle diameter	325	[µm]
Particle density	2550	[kg/m^3]
Total solid inventory	~ 25	[kg]
Bed aeration gas velocity	1.01	[u_{mf}]
V Valve aeration gas velocity	~ 13.5	[u_{mf}]
Riser aeration gas velocity	~ 13.5	[u_{mf}]
Orifice dimension	30x25	[mm]
Solids circulation rate	0.025	[kg/s]
Minimum fluidisation velocity	0.1	[m/s]
Rate: Solid Circ / Solid Inventory	0.001	[1/s]
Rate: Gas Leakage / Solid Circ Rate	-	[m^3/kg]

Table 3-3 Characteristic properties of v-valve reactor

3.4 Draft Tube Reactor

Hofbauer, H., [28] made numerous investigations on an internally circulating fluidised bed cold flow model with a 310 mm centrally located draft tube, fixed in an 865 mm high annulus section (Figure 3-6). The smaller central tube carries the particles upwards with the fluidising gas and the outer concentric tube carries the particles downwards. The effects of different solid inventories and of geometrical modifications of the apparatus on solid circulation rate and gas leakage have been determined. It was found that there is a linear correlation between solid flow and gas leakage and that the major part of gas leakage occurs from the annulus section to the draft tube in the lower part of the reactor.

Song et al. [29] determined the effects of three different gas distributors in a somewhat larger reactor and found that a circular ring sparger, located 50 mm above the bottom of the draft

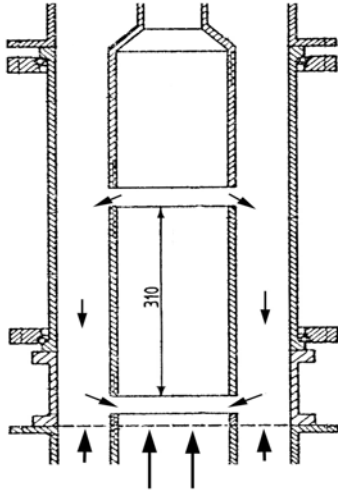tube in the annular section, provides the lowest gas bypassing, but also the lowest solids circulation rate.

Figure 3-6: Draft tube reactor [28]

Draft tube diameter	0.144	[m]
Annulus diameter	0.3	[m]
Annulus height	0.31	[m]
Average particle diameter	113	[µm]
Particle density	2640	[kg/m^3]
Total solid inventory	40	[kg]
Draft tube gas velocity	4 - 17	[u_{mf}]
Annulus gas velocity	4	[u_{mf}]
Draft tube slot height	15 -50	[mm]
Solids circulation rate	1.2	[kg/s]
Minimum fluidisation velocity	0.0175	[m/s]
Rate: Solid Circ / Solid Inventory	0.03	[1/s]
Rate: Gas Leakage / Gas Inlet	0.18	[-]
Rate: Gas Leakage / Solid Circ Rate	0.000579	[m^3/kg]

Table 3-4: Characteristic design properties of draft tube reactor

A similar gas distributor design was earlier proposed by Reichhold et al. [30] for an internally circulating fluidised catalytic cracking reactor. In recent studies Chandel et al. [31] made investigations on a spouted bed with a draft tube and presented a simple mathematical way of calculating pressure drop and gas bypassing in the circulating fluidised bed. Jeon et al [32] investigated the effects of binary solids mixtures on the gas leakage and circulation rate in a square acryl column with a centrally located draft tube. It was found that the gas bypassing fractions from the annulus section to the draft tube of binary bed materials are little higher than those of the mono-dispersed bed material.

3.5 Parallel Fluidised Beds with Transfer Tubes

Chen et al. [33] investigated the solids transfer between two identical Plexiglas columns with a diameter of 0.203m. The columns are connected via two angular transfer tubes to enable the solids circulation in the reactor system. The major objectives were to determine the possibility of attaining dense-phase (and not dilute-phase) solid transport without additional gas injection in the tubes. Furthermore, it was tried to obtain the criteria for controlling the solids transfer rate. Therefore the influence of the gas flow rate, the use of non-uniform distributor plates, the presence of internal baffles or the variation of the position of the

transfer tubes were investigated. The dependency of the solids transfer rate on these parameters can be explained in terms of the density difference of the fluidised sand.

Fercher, E. [34] used a similar but asymmetric version of the apparatus (Figure 3-7) as a cold flow model for the autothermal gasification of coal. He found that the amount of the solid circulation rate is corresponding to the diameter of the transfer tubes and that it is not influenced by the geometry of the two fluidised beds. The reason for the very low circulation rate is to be found in the small ratio between the cross sectional area and the inner surface area of the transfer tubes. Consequently, the friction forces are high between the particles and between the wall and the particles, respectively. It was also observed that electrostatic effects between the particles and the Plexiglas walls take influence on the measurements.
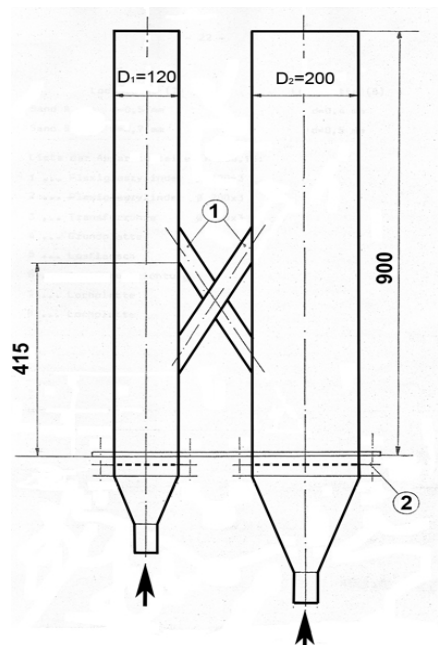

left tube diameter	0.120	[m]
right tube diameter	0.200	[m]
Reactor height	0.900	[m]
Transfer tube diameter	0.04	[m]
Average particle diameter	125	[μm]
Particle density	2630	[kg/m^3]
Total solid inventory	~30	[kg]
left tube gas velocity	10	[u_{mf}]
right tube gas velocity	10	[u_{mf}]
Transfer tube outlet height	175	[mm]
Solids circulation rate	0.0166	[kg/s]
Minimum fluidisation velocity	0.02	[m/s]
Rate: Solid Circ / Solid Inventory	0.000556	[1/s]
Rate: Gas Leakage / Gas Inlet	0.0277	[-]
Rate: Gas Leakage / Solid Circ Rate	0.0075	[m^3/kg]

Figure 3-7: Parallel FB with transfer tubes [34] ; 1….transfer tubes, 2….distributor plate

Table 3-5: Characteristic design properties of parallel FB reactor with transfer tubes.

3.6 Comparison of the Reactor Designs

In Table 3-6 the calculated values of the rates of characteristic design parameters are compared. The draft tube reactor has its main advantage in a very high circulation rate referred on the amount of solid inventory. This of course has a negative effect on the gas leakage in the system, which makes it probably more suitable for processes where the gas mixing plays a minor role. Although the rotating cone reactor delivered good values, the technical effort is found to be too high for a laboratory reactor unit. It can be assumed that

the values for gas leakage of the v-valve reactor are quite low but unfortunately no values have been delivered. Also the flexibility of the system, regarding the solid circulation rate, could be a crucial part of this reactor system. The parallel fluidised bed with transfer tubes seems to have the poorest performance amongst all, whereby its main disadvantage is clearly the low solid circulation rate. It has to be pointed out that the calculated rates of the adjacent reactor unit represent a good compromise in all three categories. This unique position represents also the aim for the planed new reactor unit.

calculated rates	$\dfrac{solid\_circulation}{solid\_inventory}$	$\dfrac{gas\_leakage}{gas\_inlet}$	$\dfrac{gas\_leakage}{solid\_circulation}$
adjacent compartment reactor	0.0083	0.0185	0.0049
rotating cone reactor	0.001	0.0252	0.0022
v-valve reactor	0.001	-	-
draft tube reactor	0.03	0.18	0.000579
parallel FB with transfer tubes	0.000556	0.0277	0.0075

Table 3-6: Comparison of calculated rates

Summed up, a comparison of the existing reactor designs led to the conclusion that the new designed reactor unit should be based on the adjacent compartment reactor concept.

4 Modification of an Existing Small-Scale Cold Flow Model

4.1 Experimental Setup

In this chapter a short overview of the setup, used for the measurements of gas leakage, solid circulation rate and the pressure profile of the laboratory reactor is given. A detailed description of the configuration of the instruments, the calibration procedure, and the software programming was made by Tagwerker, C. [35].

4.1.1 Measurement Data Logging and System Control

The computer based measurement system consists of three basic components, including the measurement software, the measurement hardware and the field bus system which enables communication between hard and software.

A LabView™ programmed front end control panel running on a laboratory PC is the interface between the user and the controlled hardware, like for example Mass Flow Controllers (MFC) or pressure transducers. The program communicates with the hardware via a FieldPoint™ field bus system, which is able to understand LabView™ commands and translates the data into a voltage-signal for the MFC. In return, the back signal of the MFC and the pressure transducers was transformed and enabled data logging during the measurements. It was also tried to implement the gas concentration measurement into the program, however, transforming the signal of the IR-spectrometer was not possible, because of the strong "drift" of the zero-point of the voltage signal.

4.1.2 Mass Flow Controllers (MFC)

For the fluidisation of the reactor system four *MKS Instruments* MFC were used. To attain correct measurement values, substantial calibration was necessary. A gas meter was used for the calibration of the large volume flows for the air reactor and the fuel reactor. The calibration of the smaller MFCs turned out to be far more elaborate, because the MFCs needed to operate at the lower control range of 0.1 l/min. For a higher accuracy a "bubble-meter" instead of the gas meter was used for the exact calibration.

MFC Type	Function	Range [l/min]
1179	fluidisation of air reactor	0.4 - 20.0
1179	fluidisation of fuel reactor	0.2 - 10.0
2179	fluidisation of downcomer	0.1 - 5.0
2179	fluidisation of slot	0.1 - 5.0

Table 4-1: Types of used mass flow controllers

4.1.3 Pressure Taps

Additionally, six *Honeywell Microswitch* pressure transducers were used to measure the pressure profile over the reactors. For the calibration of the sensors a water filled u-tube manometer was used. The manometer and the six pressure tabs were connected to a small vessel with a MFC regulated gas inlet and a pressure valve outlet. By regulating the volume flow of the MFC, the reference pressures for calibration could easily be adjusted and efficient calibration was possible. Due to a "drift" of the power supply unit of the pressure transducers, recalibration was necessary before every measurement.

Sensor Type	Function	Range [Pa]
164PC01D37	pressure measurement	0 - 2500

Table 4-2: Range of used pressure transducers

4.1.4 Gas Concentration Measurement

For the measurement of the oxygen concentrations a Rosemount NGA 2000 IR-spectrometer was used. For the control measurement in Chapter 5.4.2 methane was used a tracer gas. A Messer Griesheim Flame Ionisation Detector (FID) was used for the detection of the very small gas concentrations.

4.1.5 Powder Properties

To investigate the hydrodynamics of the system, a fine powder for Fluid Catalytic Cracking (FCC) was used as solid inventory for the cold flow model. The characteristic properties of the powder can be found in the following table:

particle diameter	d_p	70	[µm]
particle density	ρ_p	1500	[kg/m^3]
particle bulk density	ρ_b	812	[kg/m^3]
particle sphericity	ϕ	1	[-]
minimum fluidisation velocity	u_{mf}	0.00237	[m/s]
terminal velocity	u_t	0.2175	[m/s]
classification (Geldard)	group	A	[-]

Table 4-3: Characteristic properties of solid inventory

4.2 Reactor Design

The following chapter represents a compact report on the first part of this thesis. It was already mentioned above, that some improvement opportunities in the critical parts of an existing cold flow model should be implemented and lead to a better understanding of the circulating fluidised bed system.

Kronberger, B. [13] combined a set of specified process conditions and system parameters to design a 100W CLC laboratory scale unit for the combustion of fuel gas derived from the gasification of coal. The parameters contained the composition of the fuel gas, the combustion temperature, the air to fuel ratio as well as the density and mean diameter of the bed material. By applying the scaling laws of Glicksman, L. [1], it was possible to set the geometrical dimensions for the small cold flow unit which has already been introduced in chapter 3.1. Glicksman also developed two so-called reduced sets of parameters for Reynolds numbers smaller than 4 and larger than 400. As in this case, the particle Reynolds Number Re_P is well below 4, the following dimensionless numbers were held constant:

$$Fr, Re_p, \frac{L}{d_P}, \frac{D}{d_P}, \Phi, PSD, bed\_geometry \qquad (8)$$

Basically, the cold flow model consists of three parts, including the reactor section, the wind box section and the particle separator section, whereas the latter could be used for measurements on both, the original and the modified reactor. Figure 4-1 shows a comparison of the original and the modified reactor section. It can be seen that the outside geometry was not modified, due to the comparability of the results. The ramp at the end of the chute, which acts as a downcomer, was changed into a step which represents an approach to a proper J-type loop seal. A small tube was introduced into the downcomer section to fluidise the standing particle column and enable circulation.

In the slot section, two additionally mounted barriers should prevent gas leakage caused by bubbles slipping through the 1.5mm slot, due to local pressure differences between air reactor and fuel reactor. The barriers shown in Figure 4-1 (right side) have a height of 10mm on the air reactor side and 20mm on the side of the fuel reactor. The idea behind this unsymmetry was to keep the influence low on the solid circulation. The distance of each wall to the centred reactor dividing wall was 3mm. The wind-box was modified into a three compartment box, because the slot section needed extra fluidisation to maintain the circulation of the solids.
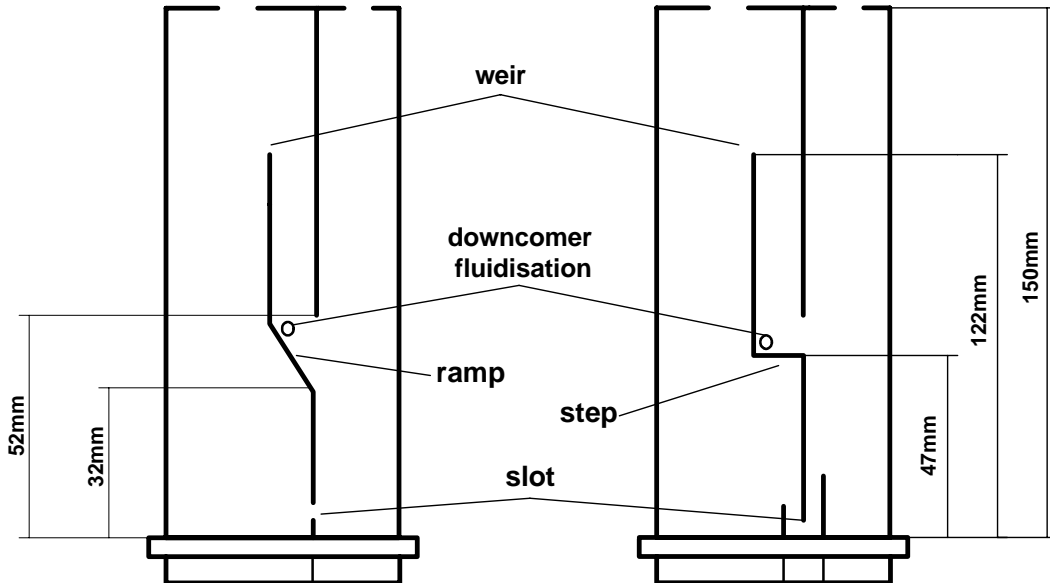
Figure 4-1: Comparison of original (left) and modified (right) reactor unit

Because of the implemented slot section the original cross sections for the AR and FR were reduced from 19x27mm and 19x19mm to 19x22mm and 19x14mm at the bottom of the reactors. In the upper part of the reactors, the geometry remained unchanged, including the height of the weir and the dimension of the downcomer (19x9mm).

4.3 Experimental

In the following chapters the results of the measurements of the modified reactor unit are presented.

4.3.1 Solids Circulation Rate

The solid circulation rate was determined by introducing a small ball into the downcomer, which was taken along by the moving solids column. When the reactor was illuminated from behind, it was possible to measure the time that the ball needed to travel down a certain distance. The ball was connected to a thin thread with which it could be pulled back to the top of the solid column. To validate the methodology, several control measurements were taken, using a very fine black powder as a tracer. Average values of a minimum of four measurements were used. For the determination of the solids circulation rate, the bulk density of the FCC powder (Table 4-3) was used in the calculation. Figure 4-2 shows that a higher fluidisation in the air reactor forces higher solid circulation rate. The volume flow has been varied between 6.59 [l/min] and 9.50 [l/min], corresponding to a superficial gas velocity of 1.4 and 2.0 u/u_t. The total solid inventory (TSI) in this case was 53g. In Figure 4-3 the

volume flow of the fuel reactor was varied between 1.54 [l/min] and 2.56 [l/min], corresponding to a minimum fluidisation velocity u_{mf} between 30 and 50. Interestingly, it was found that at a very high fluidisation rate at $50*u_{mf}$ the solid circulation decreases. It can be observed that the vivid bubbling in the fuel reactor hinders the powder to reach the narrow opening of the slot area.
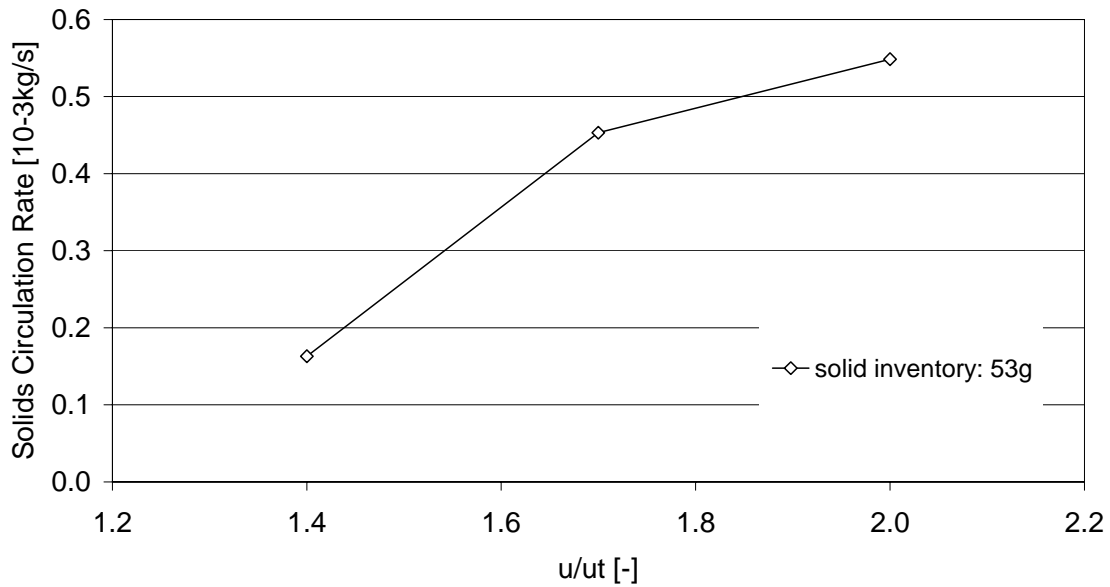

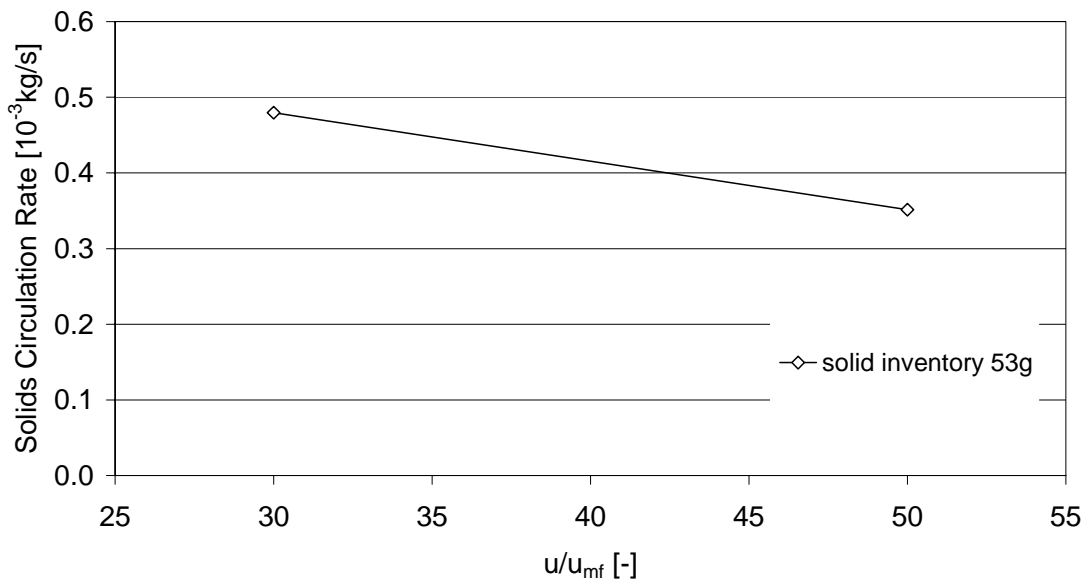**Figure 4-2: Solid circulation rate, variation of V_{AR}, V_{FR} =1.8 [l/min] = 30 u_{mf} [m/s]**

Figure 4-3: Solid circulation rate, variation of V_{FR}, V_{AR} =8.5 [l/min] = 30 u_{mf} [m/s]

It has to be mentioned that during a set of test measurements the behaviour of the FCC powder changed significantly. After introducing the powder into the apparatus it seemed to consist of agglomerations that demanded higher volume flows to form a bubbling fluidised bed than a loose powder. This behaviour was independent on the gas, which was used for the fluidisation. The bubbling inside the reactor was easy to inspect because the acrylic glass remained clear and did not form an adhesive bond with the particles. After several hours of constant fluidisation, however, the powder seemed to have lost the agglomerations and formed a significantly denser freeboard zone above the bubbling bed. Additionally, it could be observed that a thin layer of particles was settled over the reactor walls, which obviously had strong influence on the fluidisation behaviour. Numerous investigations including drying and microscopic inspections of the powder as well as antistatic grounding of the apparatus led to the assumption that the wall effects are responsible for the changing fluidisation behaviour and the resulting variations in the measured circulation rate.

To avoid the above mentioned effects, "fresh" powder that had been introduced into the reactor, had to be fluidised for several hours before a reproducible measurement could be achieved.

4.3.2 Gas Leakage

For the determination of the gas leakage between the air reactor and the fuel reactor a simple tracer-method was used. Nitrogen and air were used for the fluidisation of the reactors, whereas the ambient air with an average oxygen fraction of 21 vol%, was used as the tracer gas. To determine the leakage from the AR to the FR, the AR was fluidised with air and the oxygen fraction at the fuel reactor outlet was measured. Via a mass-balance over the total system the split of the gas streams could be determined. In Figure 4-4 a black-box model of the system is presented.
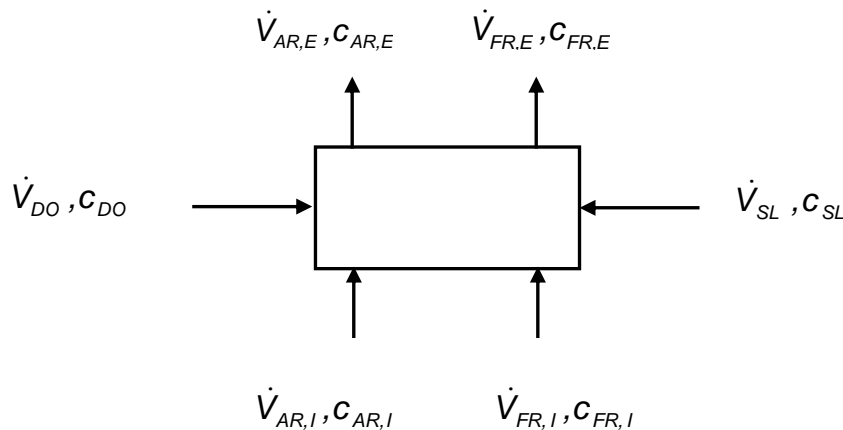

Figure 4-4: Black-box model of the reactor system

With the total balance over the reactor

$$\dot{V}_{AR,E} + \dot{V}_{FR,E} = \dot{V}_{AR,I} + \dot{V}_{FR,I} + \dot{V}_{DO} + \dot{V}_{SL}$$

and the oxygen mass balance

$$\dot{V}_{AR,E} * c_{AR,E} + \dot{V}_{FR,E} * c_{FR,E} = \dot{V}_{AR,I} * c_{AR,I} + \dot{V}_{FR,I} * c_{FR,I} + \dot{V}_{DO} * c_{DO} + \dot{V}_{SL} * c_{SL}$$

the exit volume flows $\dot{V}_{AR,E}$ and $\dot{V}_{FR,E}$ can be calculated:

$$\dot{V}_{AR,E} = \frac{\dot{V}_{AR,I}\left(c_{AR,I} - c_{FR,E}\right) + \dot{V}_{FR,I}\left(c_{FR,I} - c_{FR,E}\right) + \dot{V}_{DO}\left(c_{DO} - c_{FR,E}\right) + \dot{V}_{SL}\left(c_{SL} - c_{FR,E}\right)}{\left(c_{AR,E} - c_{FR,E}\right)}$$

$$\dot{V}_{FR,E} = \dot{V}_{AR,I} + \dot{V}_{FR,I} + \dot{V}_{DO} + \dot{V}_{SL} - \dot{V}_{AR,E}$$

As shown in Figure 4-5, the unwanted gas stream through the downcomer is defined as "dilution" and the stream of gas through the slot on the bottom of the reactor is defined as "leakage".
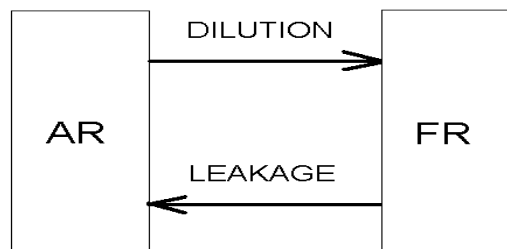
Figure 4-5: Definition of gas leakage

To attain a percental designation of the measured values, the measured leakage gas stream of one reactor, was referred to the inlet volume flow of the other reactor, and vice versa.

The following equations were used for the calculation of the results:

$$DILUTION = \frac{\left(\dot{V}_{FR,E} * c_{FR,E} - \dot{V}_{FR,I} * c_{FR,I}\right)}{\dot{V}_{AR,I} * c_{AR,I}}$$

$$LEAKAGE = \frac{\left(\dot{V}_{AR,E} * c_{AR,E} - \dot{V}_{AR,I} * c_{AR,I}\right)}{\dot{V}_{FR,I} * c_{FR,I}}$$

The gas leakage was measured and plotted against the variation of the air reactor velocity and the fuel reactor velocity, respectively (Figure 4-6 and Figure 4-7). It can be seen that the leakage rises when the volume flow of the air reactor is increased. This behaviour is closely related to the higher solid circulation rate in the system. In a second measurement the influence of the fluidisation rate in the downcomer and in the slot section is investigated. It was found that increasing the fluidisation rate from 0.1 [l/min] to 0.2 [l/min] reduces the leakage, although is has no influence on the circulation rate of the solids. A "stripping effect" of the fluidisation gas, which prevents leakage gas from streaming along with the powder, is a possible explanation for the lower leakage values. However, it has to be mentioned that a fluidisation rate of 0.2 [l/min] corresponds to a minimum fluidisation velocity of approximately 12.3 u_{mf} in the slot section, which is a very high value compared to a industrial loop seal, and therefore represents an unusual way to reduce the gas leakage. Increasing the volume flow in the fuel reactor does not have an effect on the gas leakage, regarding absolute values. In a percental designation like it is depicted in Figure 4-7 the leakage decreases, because the absolute values are referred on the higher fuel reactor volume flow.
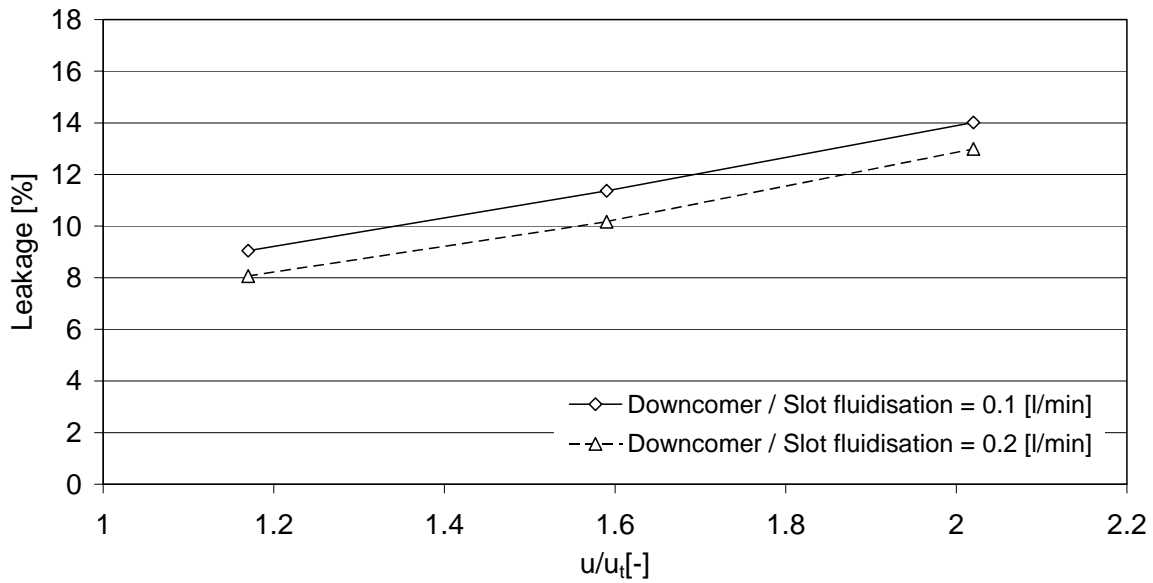
Figure 4-6: Leakage into air reactor, slot height 1.5 mm, variation of V_{AR}, V_{FR} = 1.54 [l/min] = $30*u_{mf}$ [m/s]

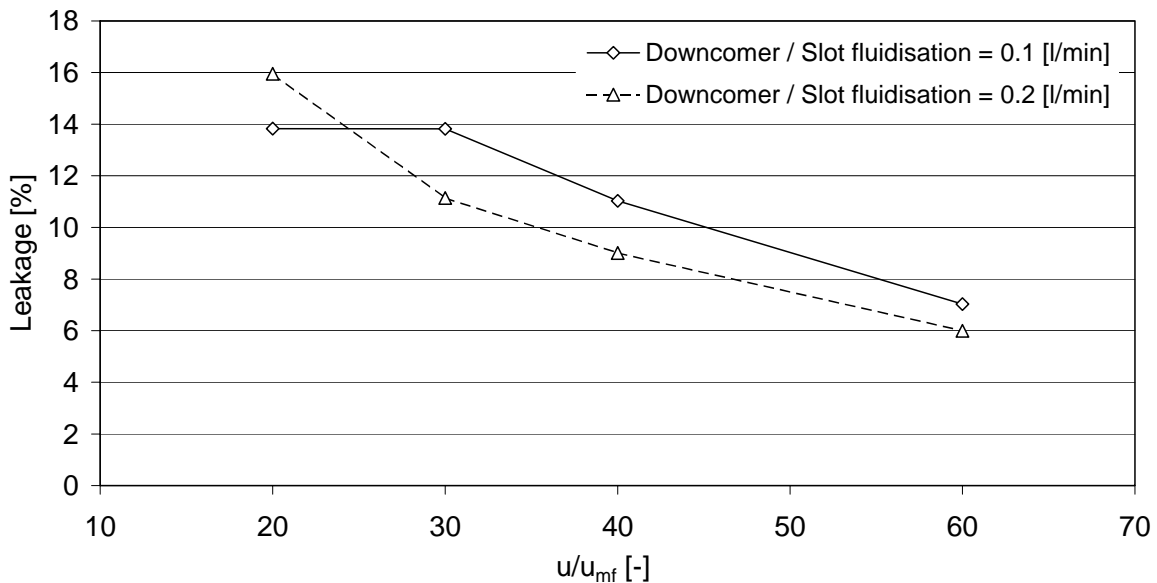**Figure 4-7: Leakage into air reactor, slot height 1.5 mm, variation of V_{FR}, V_{AR} = 8.5 [l/min] = $1.8*u_t$ [m/s]**

The measured values for the dilution were significantly lower than the leakage values. Figure 4-8 demonstrates a very interesting behaviour of the reactor system. When the fluidisation rate of the fuel reactor is decreased below 30 u_{mf}, the dilution suddenly rises from only 0.3% to about 4%.

27

It is likely that the main mechanism of the dilution is the exchange of gas bubbles reaching accidentally the other reactor through the slot and not the downcomer. In earlier measurements (Figure 4-3) it was found that increasing the fuel reactor velocity significantly decreases the solid circulation rate. It could be observed that in this case more solid inventory is accumulated in the fuel reactor, which increases the pressure in the fuel reactor. The counter pressure prevents the exchange of gas bubbles and the dilution drops down to a value of approximately 0.5%.
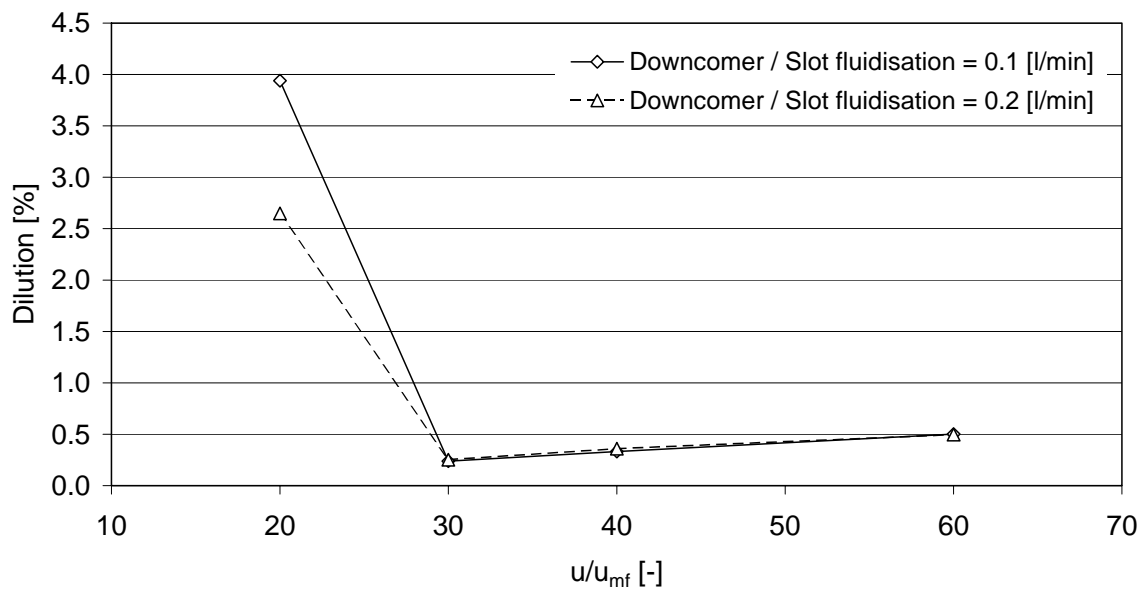
Figure 4-8: Dilution into air reactor, slot height 1.5 mm, variation of V_{FR} , V_{AR} = 8.5 [l/min] = 1.8*u_t [m/s]

4.3.3 Pressure Profile

The previous chapter clarified, that the pressure balance of the CFB system needs careful consideration. However, measurements on the small scale cold flow model were difficult and reproducible values were hard to attain. Beside a systematic failure caused by the drift of the pressure transducers, plugging of the pressure taps caused inaccurate measurements. The presented values in Figure 4-9 represent average values from a minimum of five measurements.

The pressure profile over the reactor height was measured at an air reactor volume flow of 8.5 [l/min], which corresponds to 1.8 u_t and the fuel reactor velocity was set to 1.54 [l/min], which corresponds to $30u_{mf}$. It can be seen that at the height of the downcomer return orifice (47-53mm) the pressure in the AR is higher than in the FR. Measuring the pressure at bottom of the reactors was not possible because of strong pressure fluctuations. By prolonging the lines of the pressure profiles in Figure 4-9 to the abscissa, a pressure difference in the range of 400 to 600 Pa can be interpolated. This pressure difference is also the driving force for the solid circulation from the fuel reactor to the air reactor.
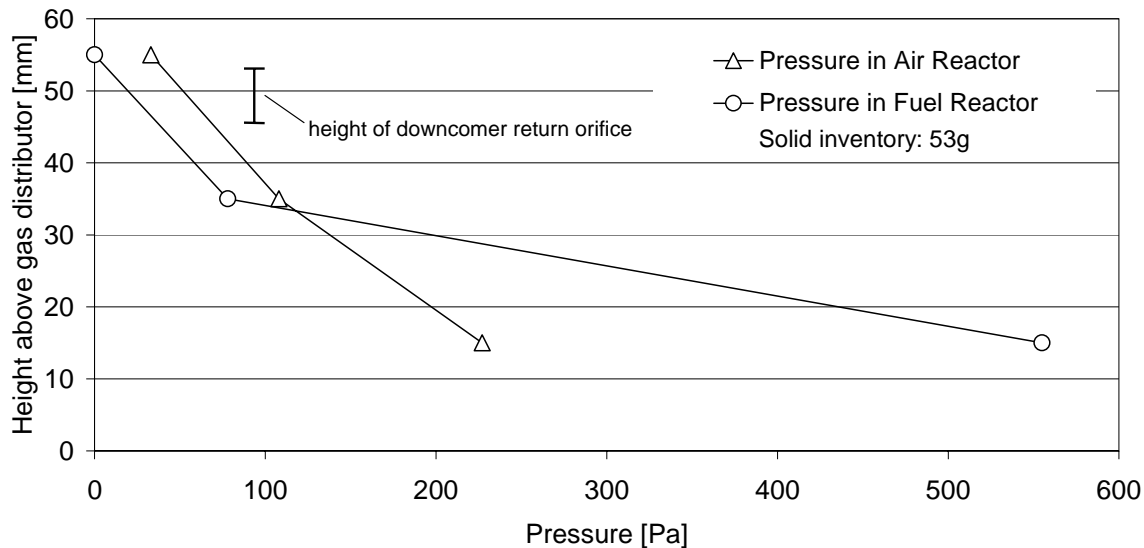

Figure 4-9: Pressure profile over reactor height, solid inventory 53g, V$_{AR}$ = 8.5 [l/min] = 1.8 u$_t$; V$_{FR}$ = 1.54 [l/min] = 30u$_{mf}$.

To investigate the applicability of the reactor system to CLR operating conditions, a second pressure profile was created, by introducing less solid inventory into the reactor system. As a result, the pressure in both reactors is lower and that there is no intersection of the pressure profiles in the reactors. This means that at the height of the solids return orifice the pressure

in the fuel reactor is somewhat higher than in the air reactor. It could be observed that this counter pressure was compensated by a higher particle column in the downcomer section. Again, an interpolated pressure difference between 350 to 500 Pa at the bottom of the two reactors is the driving force for the circulation through the slot.
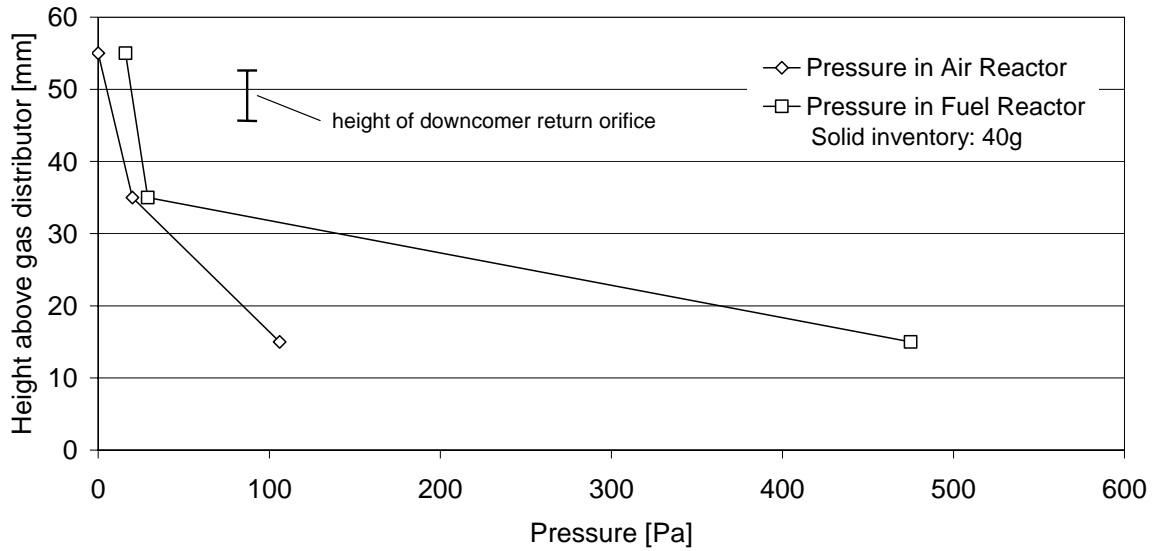

Figure 4-10: Pressure profile over reactor height, solid inventory 40g, V_{AR} = 8.5 [l/min] = 1.8 u_t; V_{FR} = 1.54 [l/min] = 30u_{mf}.

5 Investigation of a Mid-Scale Cold Flow Model

5.1 General Design Issues

In this section, the attained knowledge of the small laboratory unit should be applied in a newly constructed reactor design at a slightly larger scale. The main argument for the change in scale, were the aforementioned significant wall effects detected during the work with the small-scale unit. The geometry scale was increased by a factor of two for all dimensions and so the new unit has a much closer geometry ratio (e.g. d_p/D) to a large scale "hot" reactor, than the previous unit. For this reason the newly constructed reactor design is expected to deliver valuable experimental results.

5.2 Experimental Setup

The setup is very similar to the setup used with the small-scale model described in Chapter 4.1. For the higher volume flow in the air reactor a 100l/min MFC (100.000sccm) has been installed and the 20l/min MFC that was formerly used for fluidising the air reactor was installed for the fluidisation of the fuel reactor. Again, the volume flow in the downcomer- and in the slot-section was set to 0.1 l/min, which corresponds to a minimum fluidisation velocity of approximately $1.8 \cdot u_{mf}$, assuming an equal split of the fluidisation gas into the two reactors.

5.3 Reactor Design

To increase the accuracy in the executed measurements and to reduce the influence of the reactor-walls, such as friction and possible electrostatic effects deriving from the constantly fluidised powder shearing on the acrylic glass wall, a larger reactor design was chosen for further investigations. Figure 5-1 shows the three main parts of the cold flow model representing the reactor section, the cyclone section and the wind box section, resulting in a total height of 770mm. The three units are connected by flanges with appropriate rubber sealings and silicon paste to extinguish any unwanted leakages that could influence the measurements. So the apparatus can be dismantled for modifications on at least some parts of the inside geometry.
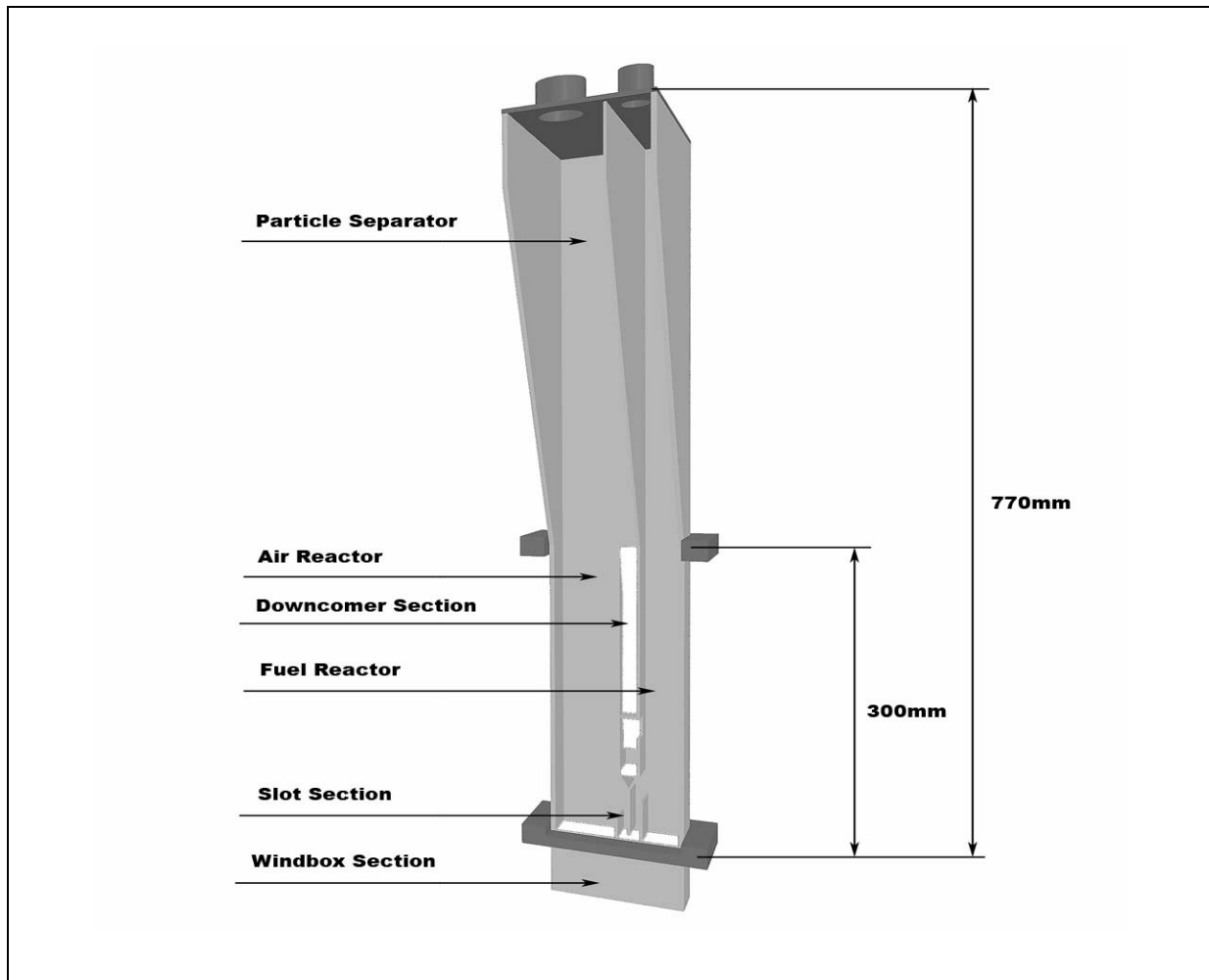
Figure 5-1: Main parts of the cold flow model (front view)

5.3.1 The Reactor Section

The height of the reactor unit is 300 mm. It is divided into the air reactor with a base area of 50 x 30 mm, the fuel reactor with a base area of 30 x 30 mm and a central part, the downcomer section. This is the path that the particles follow from the air reactor to the fuel reactor (see Figure 5-2). The design of the downcomer is similar to that of a J-type loop seal and consists of one channel (14 x 14 mm) through which the particles coming from the particle separator flow downwards and a second parallel channel (14 x 14mm) through which the particles flow upwards and then over a weir into the fuel reactor. The two channels are interconnected via a small vertical orifice (20 x 14mm) and are fluidised from beneath by a
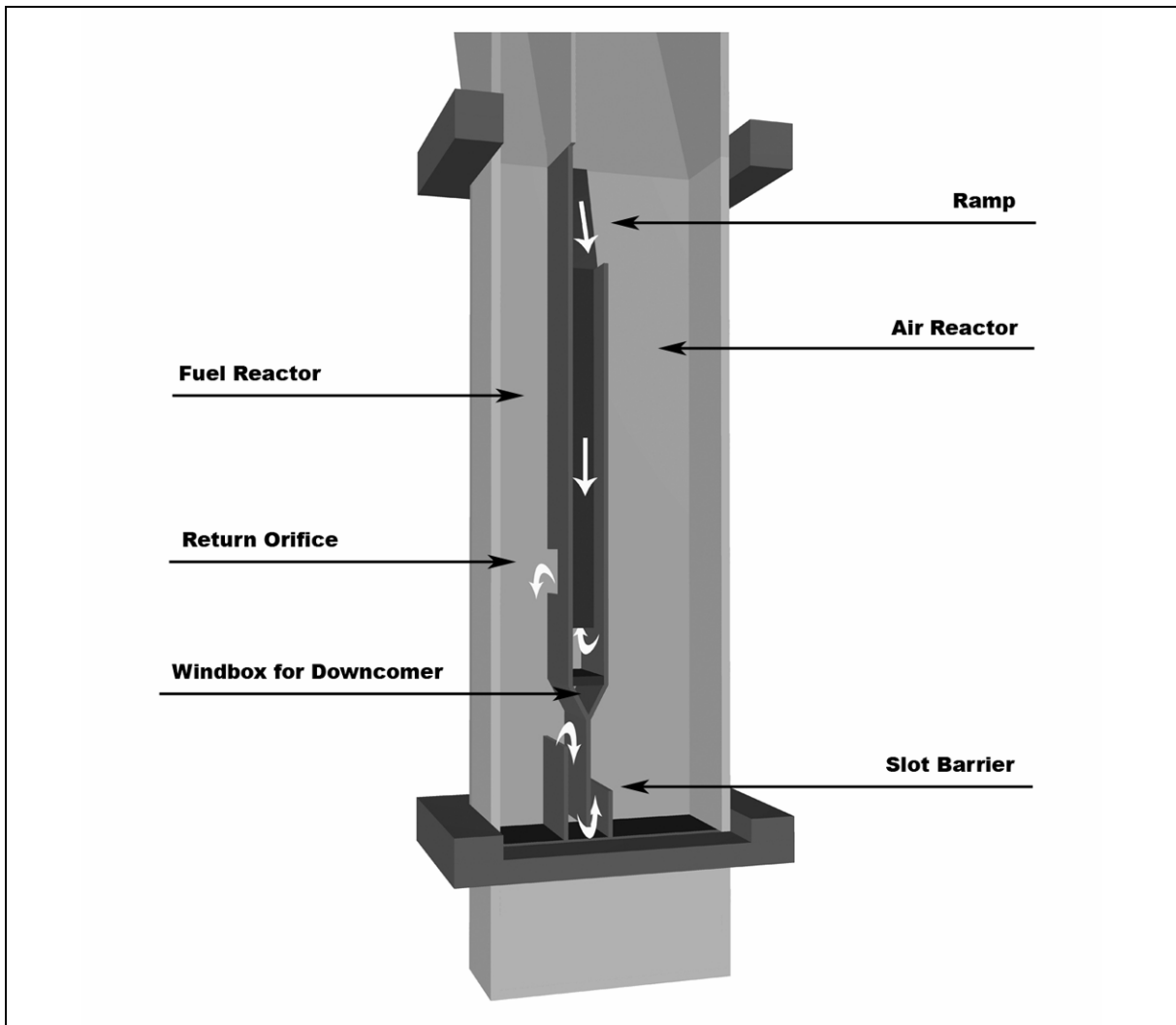
Figure 5-2: Flow of solid inventory in the reactor (rear view)

small porous plate sitting on top of a small triangle shaped wind box that is supplied with the fluidisation gas through a connection in the outer reactor wall. In comparison to the orifice area of the slot section, the downcomer area seems to be a bit over dimensioned, but with respect to possible plugging of the downcomer and the fact that it can not be dismantled, this seemed to be a good solution. Also, the widths of the air- and fuel reactor do both not influence that function of the loop seal, and the return orifice respectively, and may be altered later. In this case, clearly, the results of leakage tests need to be transferred accordingly.

The major improvement of this rather complex geometry is that a comparatively small amount of solid inventory is needed to "lock" the siphon. Also, the level of the standing particle column of the fluidised solids in the downcomer is limited by the weir and therefore expected to be constant. The u-shaped "particle-lock" design should minimize the dilution

from the air reactor to the fuel reactor to the order of magnitude of the interparticle void ε, which is transferred through the orifice together with the transported solid inventory.

5.3.2 The Wind Box Section

The wind box section consists of three adjacent chambers, each of them with a porous plate on top serving as distribution plate with sufficient pressure drop for appropriate fluidisation of the solid inventory. The chambers are separated by two walls that are elongated into the
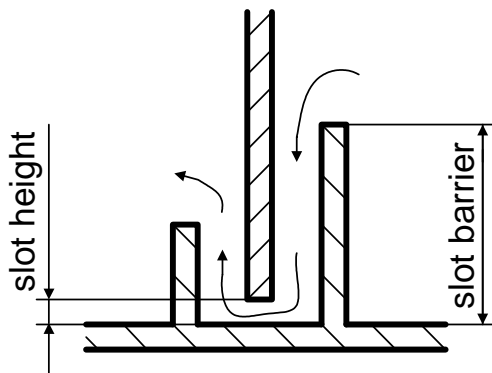
Figure 5-3: Detailed view of the slot area

reactor unit to separate the air reactor fluidisation, the fuel reactor fluidisation and the fluidisation in the slot section (centre) and avoid mixing of gas and solids. As can be seen in Figure 5-2 the height of the two walls confining the slot area was held constant at 40 mm on the side of the fuel-reactor and 20 mm on the side of the air-reactor during the first set of experiments. When attached to the reactor unit, the two walls are divided by a third wall from above, representing the slot, leaving only a small orifice to let the particles pass through (see Figure 5-3). The whole design represents a barrier for the

particles, and again it is attempted to be similar to a J-type loop seal, except that it is realised in a very compact approach. During the first set of experiments the height of the centred wall has been varied corresponding to a slot height of 5mm, 3mm and 1.5mm.

5.3.3 The Particle Separator Section

To reduce the particle velocity, a conical box was attached on top of the reactor setting the gas velocity to 0.09 m/s, which is less than the half of the terminal velocity of the 60 μm-diameter particles. This forces the particles to settle down on the ramp and then fall into the downcomer channel. Due to the design geometry, approximately only one fifth of the settled particles reach the channel, whereas the rest falls back into the bed. Therefore, it can be assumed that certain geometrical fixtures mounted on the ramp, which lead the particles into the downcomer, could increase the solid circulation rate significantly, which was earlier proposed by Kronberger, et al. [13].

5.4 Experimental

In the following chapters the results of the measurements are presented. During the first set of measurements, the solids circulation rate and the influence of the slot height on the gas leakage was analysed. Therefore the slot-height was varied between 5.0 mm, 3.0 mm and 1.5 mm. Also the amount of solid inventory was varied between 100g, 150g and 200g, corresponding to different operating states in a hot laboratory unit, like e.g. chemical looping reforming, which requires less solid inventory, because of under-stochiometric oxygen supply.

With the experience of these measurements some modifications on the geometry of the cold flow model were made. The height of the barrier confining the slot area on the air reactor side was increased from 20 mm to 40 mm. Also, the two parallel channels of the downcomer were elongated from 40 mm to 60 mm to investigate the effects of the modifications on the gas leakage in the reactor (see Chapter 5.4.2). Table 5-1 shows the experimental program and gives an overview of the varied parameters during the measurements.

model configuration	measurement of	slot [mm]	solid inventory [g]	u_{AR} ($=x^*u_t$) [m/s]	u_{FR} ($=x^*u_{mf}$) [m/s]
no modification	solid circulation rate	1.5;	100; 150; 200;	1.08; 1.2; 1.32; 1.44;	20; 60; 100;
		3.0; 5.0;	100; 150; 200;	1.2; 1.6; 2.0;	20; 40; 60;
	leakage	1.5; 3.0; 5.0	100; 150; 200;	1.2; 1.6; 2.0;	20; 40; 60;
	dilution	1.5; 3.0; 5.0	150; 200;	1.2; 1.6; 2.0;	20; 40; 60;
	pressure profile	1.5;	100; 150;	1.6;	20;
downcomer modification	dilution	1.5;	100; 150; 200;	1.2; 1.6; 2.0;	20;
slot boundary modification	dilution	1.5;	100; 150; 200;	1.2; 1.6; 2.0;	20;
	leakage	1.5;	100; 150; 200;	1.2; 1.6; 2.0;	20; 40; 60;
	solid circulation rate	1.5;	100;	1.6; 2.0;	20;
		1.5;	150; 200;	1.2; 1.6; 2.0;	20;

Table 5-1: Overview on parameter variations during experimental program

5.4.1 Solids Circulation Rate

For the results presented in Chapter 4.3.1, a thin thread with a ball that indicated the position of the powder travelling through the downcomer was used for measuring the solid circulation rate. This technique could not be applied for measurements on the redesigned cold flow model, because of the specific design of the downcomer section. As already mentioned above, the level of the surface in the u-shaped siphon-like construction was limited by the height of the weir. Therefore, the measured length was too short to produce reliable values. It seemed to be a good and simple solution to measure the time that the powder needs to fill

up the downcomer to a certain level, after stopping the fluidisation in this section. The effect that some of the solid inventory was stored in this section and therefore lacking the circulating system during the measurement was found to be negligible.

In Figure 5-4 and Figure 5-5 the specific solid circulation rate G_s is plotted against the velocities in the air reactor and in the fuel reactor respectively. To compare the values with other circulating fluidised beds, G_s is referred to the base area of the air reactor and values in a range between 0.04 and 1.5 kg/sm^2 could be measured. Significantly higher values are accomplishable if geometrical fixtures, that lead the powder into the downcomer, are installed in the particle separator section (see Chapter 5.3.3).

It can be seen that the fluidisation velocity of the air reactor controls the circulation rate. An influence of the fuel reactor fluidisation velocity could not be found at this comparatively high fluidisation velocities in the fuel reactor between 20 and $100*u_{mf}$. Furthermore, the amount of introduced solid inventory seems to have a stronger effect on the circulation than a variation of the slot height. Due to a calculation failure the values of the 1.5 mm slot are only measured up to a fluidisation velocity of $1.44*u_t$, but further measurements on the modified apparatus with the 1.5mm slot height are presented later.

In Figure 5-6 and Figure 5-7 the specific solid circulation rate is again plotted against the fluidisation velocities of the two reactors, whereas it is no longer referred on the base area of the reactor, but on the area of the slot orifice and named F_s. It can bee seen that the smallest slot area is capable to guide through the highest specific mass of fluidised powder. This behaviour has also been observed in earlier experiments, e.g. Hofbauer, H. [28], Kronberger et al. [13], Johansson et al. [14], Fang, et al. [17]. It is clear that further decreasing of the slot height would lead to a maximum in the solids throughput and then drop down to zero. However, experiments were not satisfying and could not deliver reliable values. At a slot height of 1 mm the solid circulation stopped completely and increasing it back to 1.2 mm induced to an unsteady behaviour, depending on the initial mass distribution between the reactors. Cyclic operation regarding the solid circulation rate and hysteresis effects that have been observed by Leung et al. [25] are possible but have not been investigated in this thesis.

One possible reason for the locking of the slot could be that the fluidisation gas that flows through the distributor plate right beneath the narrow slot, hinders the fluidised powder to pass through to the other reactor. A non-fluidised area on the distribution plate in this section could enable a smaller slot height, without the above mentioned effects.
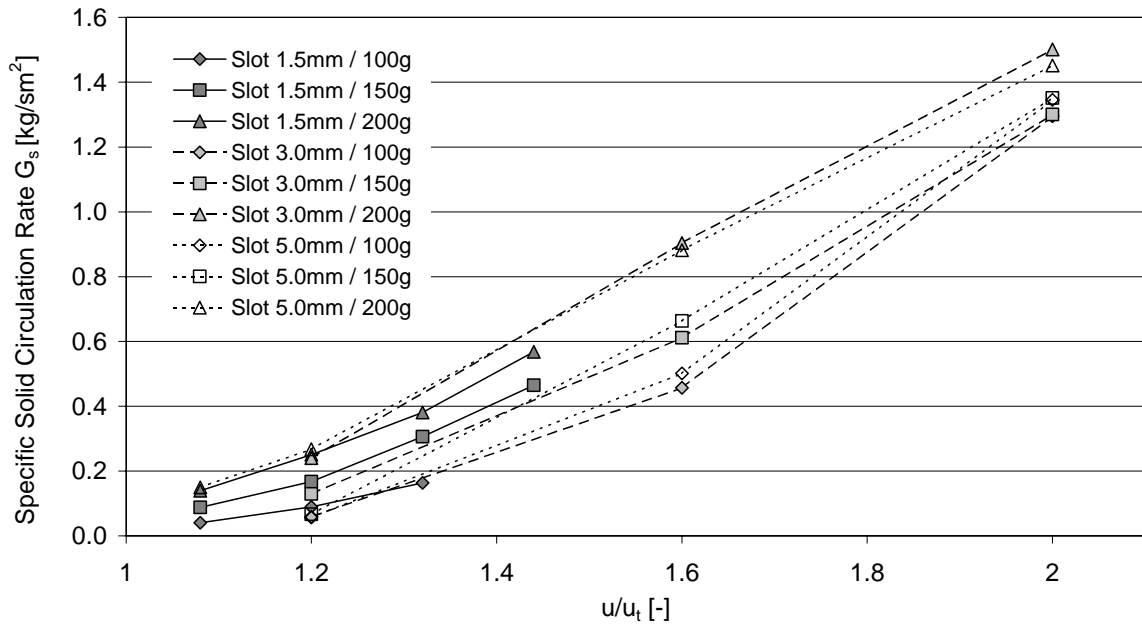
Figure 5-4: Specific solid circulation rate G_S referred to A_{AR}, variation of V_{AR}, V_{FR} = 7.68 [l/min] = $60u_{mf}$ [m/s]
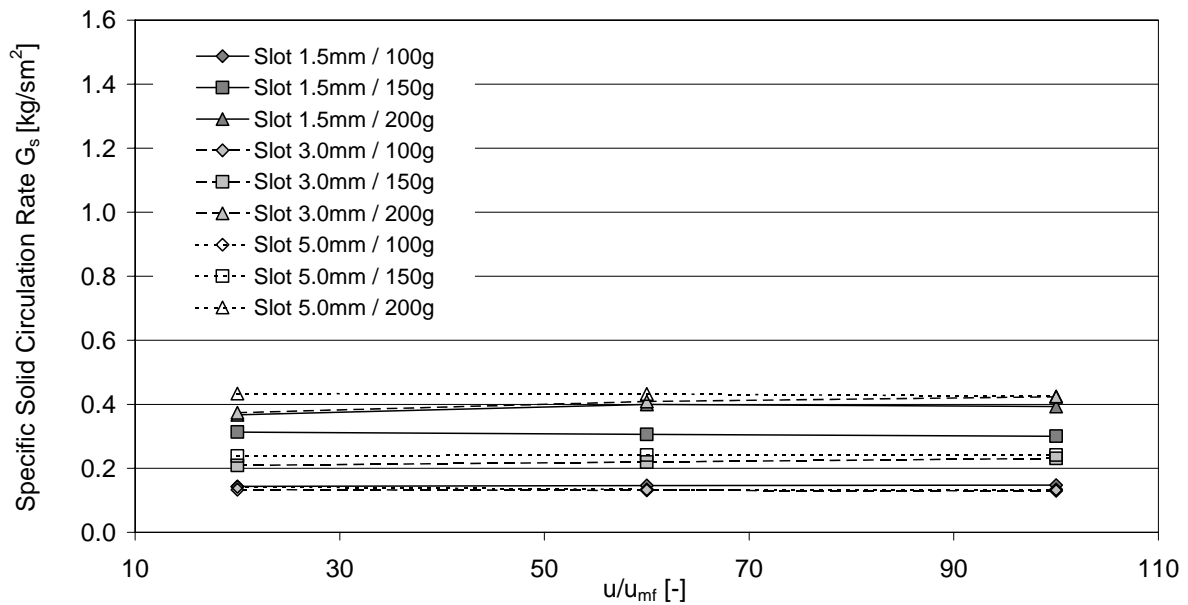

Figure 5-5: Specific solid circulation rate G_S referred to A_{AR}, variation of V_{FR}, V_{AR} = 25.84 [l/min] = 1.32 u_t [m/s]
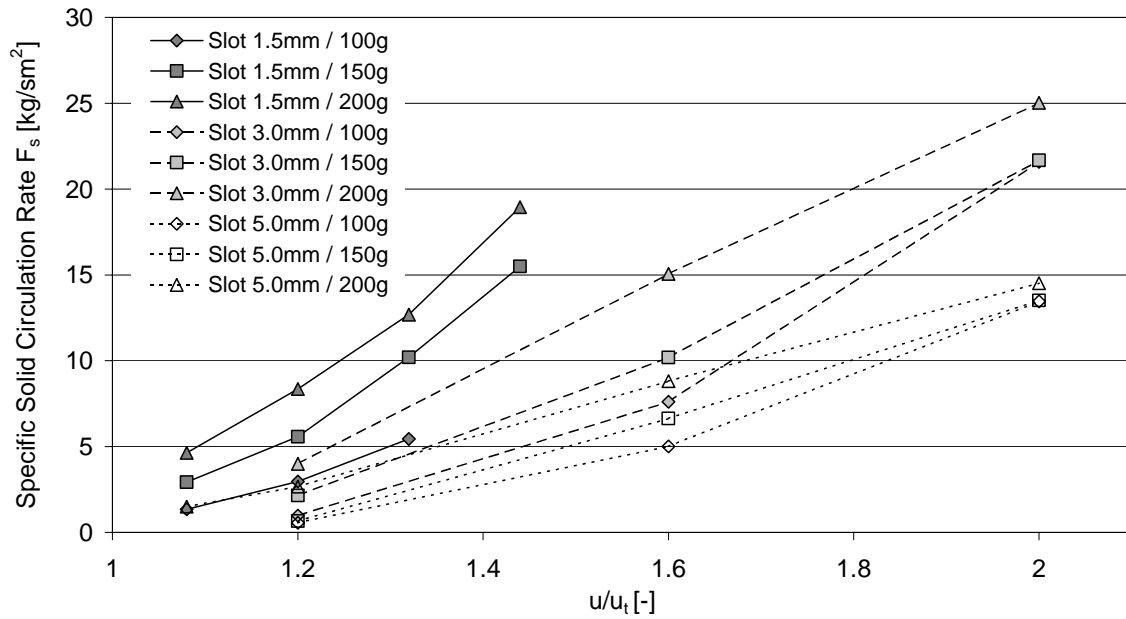
Figure 5-6: Specific solid circulation rate F_S referred to A_{Slot}, variation of V_{AR}, V_{FR} = 7.68 [l/min] = 60u_{mf} [m/s]
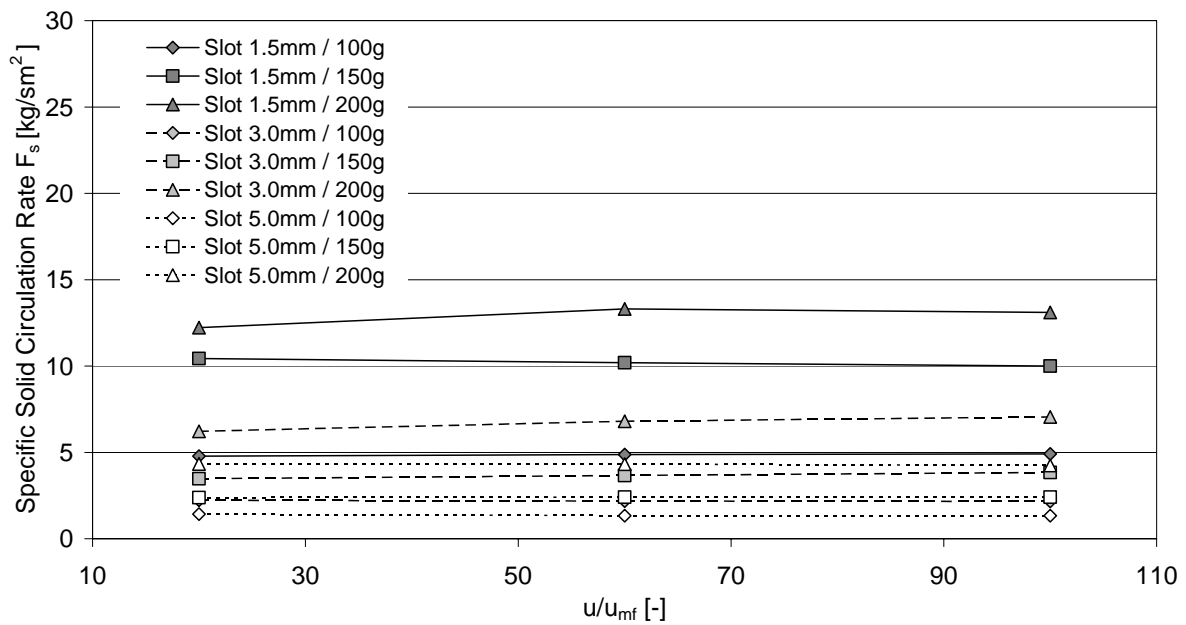

Figure 5-7: Specific solid circulation rate G_S referred to A_{Slot}, variation of V_{FR}, V_{AR} = 25.84 [l/min] = 1.32 u_t [m/s]

Modification of the Cold Flow Model

After the design of the reactor was changed some interesting results could be achieved. In Figure 5-8 the specific solid circulation rate G_s is plotted against the air reactor velocity of the modified reactor (dotted line) and also the original reactor (solid line). Apparently the changes did not have a strong effect on the circulation rate at higher solid inventories, but the values seem to be more expanded at lower solid inventories. Obviously the lacking of the solid inventory in the cycle takes effect on the circulation rate. It was calculated that approximately 17-25 g are trapped in the enlarged downcomer and also in the heightened slot boundary area. Also, the fact that at the lowest solid inventory and lowest air reactor velocity no re-producible values could be accomplished, supports the theory that too less powder remains in the circle. The chain dotted line in Figure 5-8 represents corrected values of G_s after compensating the lack of solid inventory by linear approximation of the measured values.

It can be seen that corrected values match better with the measurements of the original design. However, the modifications of the reactor have a stronger effect on solid circulation rate, when less solid inventory is introduced into the reactor.
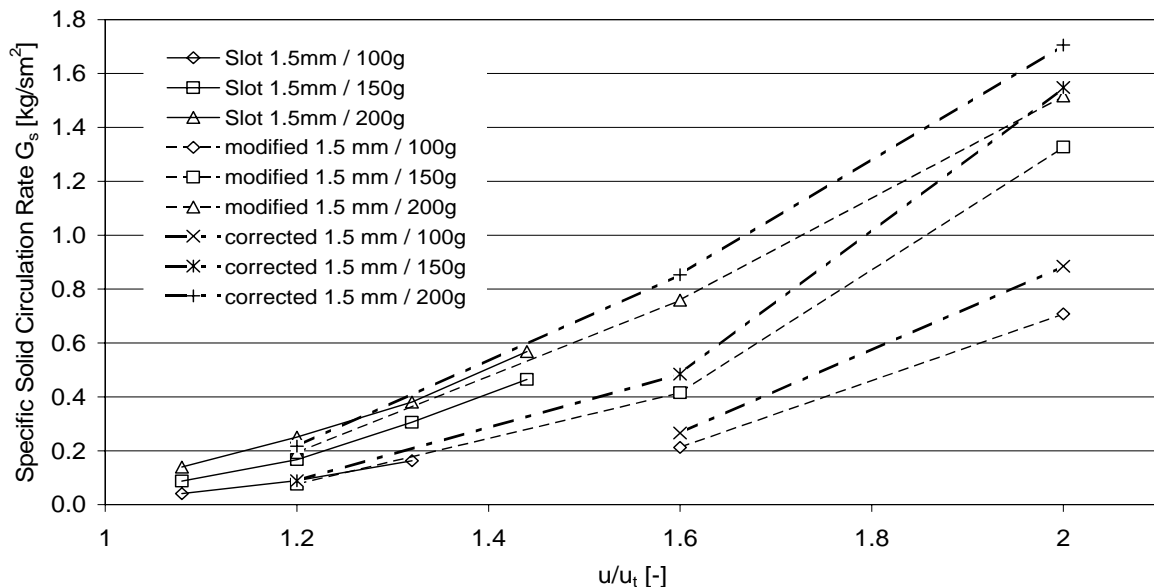

Figure 5-8: Specific solid circulation rate G_S, variation of V_{AR}, modified apparatus, V_{FR} = 7.68 [l/min] = 60u_{mf} [m/s]

5.4.2 Gas Leakage

The gas leakage was measured and plotted against the variation of the air reactor velocity and the fuel reactor velocity, respectively. Again, the unwanted gas stream through the downcomer is defined as "dilution" and the stream of gas through the slot on the bottom of the reactor is defined as "leakage". As already mentioned above, dilution of the fuel reactor exit gas stream would increase the costs for compression and the leakage into the air reactor would produce a loss in the CO_2 capture efficiency.

Kronberger et al. [13], Johansson et al. [14] and Rydén, et al. [12] showed that the amount of dilution is significantly smaller than the amount of leakage. It was assumed that the higher pressure gradient on the bottom between the fuel reactor and the air reactor, which is the driving force for the solid transport through the slot, causes the higher gas leakage. Also the existence of gas bubbles that slip through the orifice, due to local pressure drops on both sides of the slot was mentioned as a possible reason for the higher leakage values. Additionally, the downcomer of the small unit, which consists of a long channel with a dense particle column acting as a "gas-lock", seemed to work properly although only the pressure gradient between the reactors held the column at its position. The additionally mounted barriers in the slot area of the new cold flow model are therefore expected to minimize the above-mentioned effects.

Variation of the Slot Height

In the following figures for measurements with the 5 mm slot some clear trends are recognisable: The leakage from fuel reactor to air reactor seems to be around zero, whereas the dilution into the fuel reactor is very high and in the range of 0.1 to 0.45 l/min, depending on the fluidisation of the air reactor and on the amount of solid inventory.

The measurements with the 3mm slot show nearly the same trend, besides a somewhat lower dilution in the range of 0.02 to 0.3 l/min.

With regard to the observations these values seem to be false. A dilution flow of 0.45 l/min in the downcomer section would lead to a vivid bubbling of the bed on the side of the weir, which could not be observed. It was found that the strong fluidisation in the air reactor resulted in a very turbulent bubble regime right above the slot boundary, which produced a steady bubbling through the orifice into the fuel reactor. Because of the stripping effect of the

gas stream through the powder and the high dilution of the leakage gas with the air reactor gas stream, no leakage was measured (see Figure 5-13 and Figure 5-14).

The measured amount of leakage gas through the 5 mm slot (Figure 5-9 and Figure 5-10) could be connected with the reasonably higher solid circulation rate that transports a larger amount of gas into the air reactor. It was tried to calculate the amount of gas that is transported in the interparticle void along with the solid flow. It was found that a maximum of approximately 0.075 l/min are transferred into the air reactor, compared to a measured leakage of about 0.06 l/min. Therefore it can be stated that parts of the gas are stripped back into the fuel reactor.

After decreasing the slot height to 1.5 mm some very good results could be obtained. Obviously, the narrow orifice prevented the bubbles from slipping through to the fuel reactor and the leakage gas flow is in the range of 0.07 to 0.23 l/min (see Figure 5-17). Along with the increasing leakage the dilution decreased significantly, which is a good proof for the earlier assumptions. Figure 5-19 and Figure 5-20 show that the measured dilution is now in a range of 0 to 1.2 l/min which is a very reasonable value.
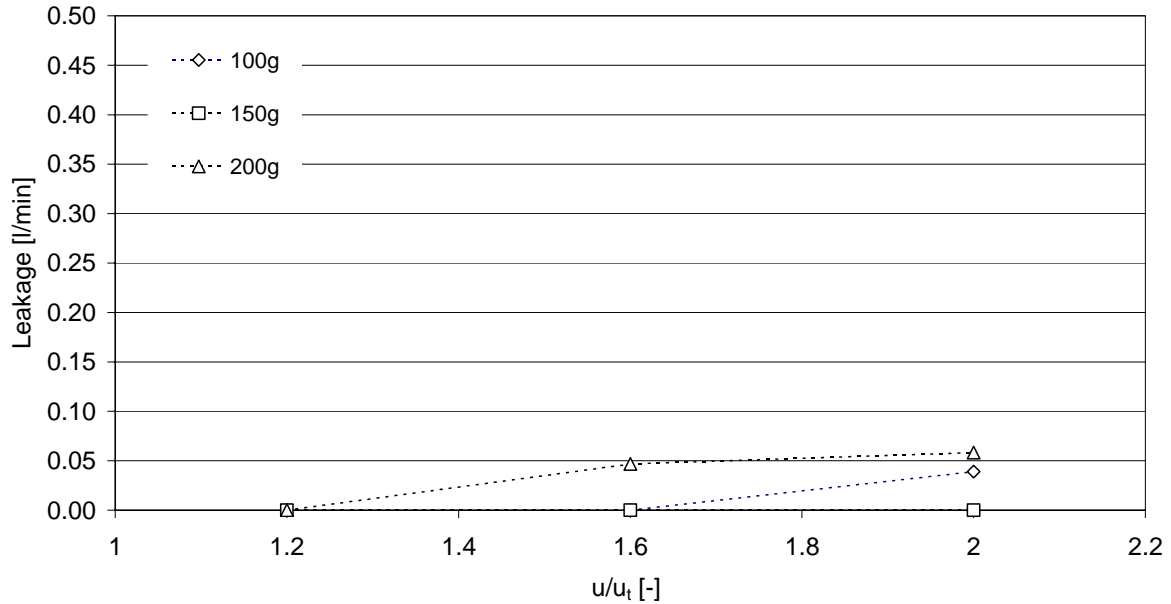
Slot Height 5.0mm:

Figure 5-9: Absolute leakage into air reactor, slot height 5 mm, variation of V_{AR}, V_{FR} = 2.56 [l/min] = 20*u_{mf} [m/s]
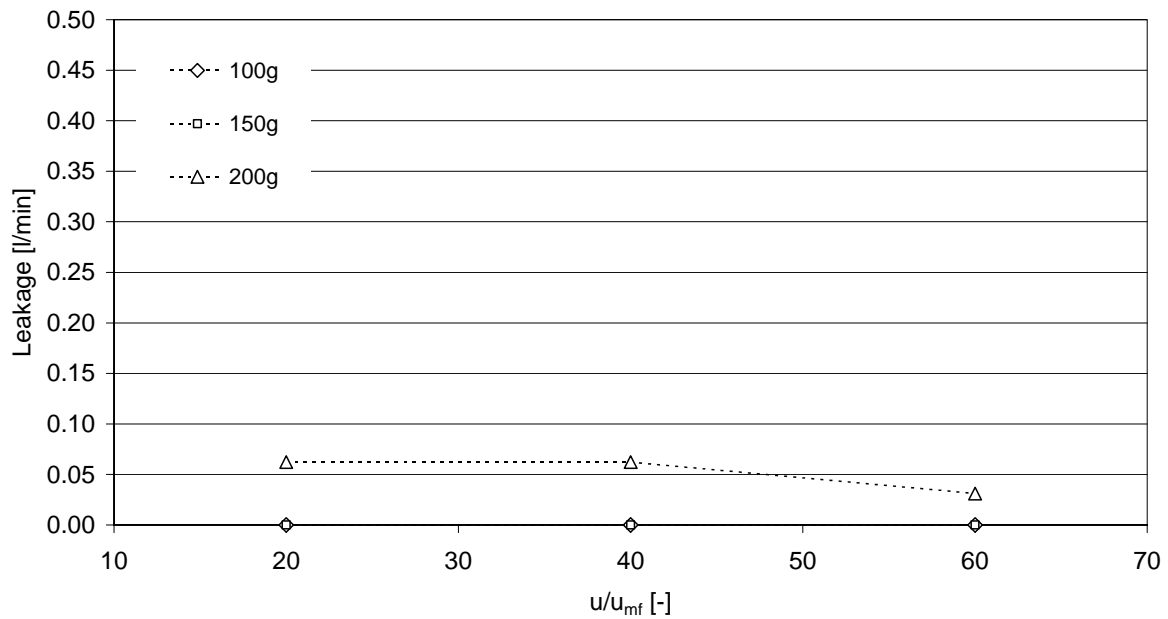

Figure 5-10: Absolute leakage into air reactor, slot height 5 mm, variation of V_{FR} , V_{AR} = 31.32 [l/min] = 1.6*u_t [m/s]
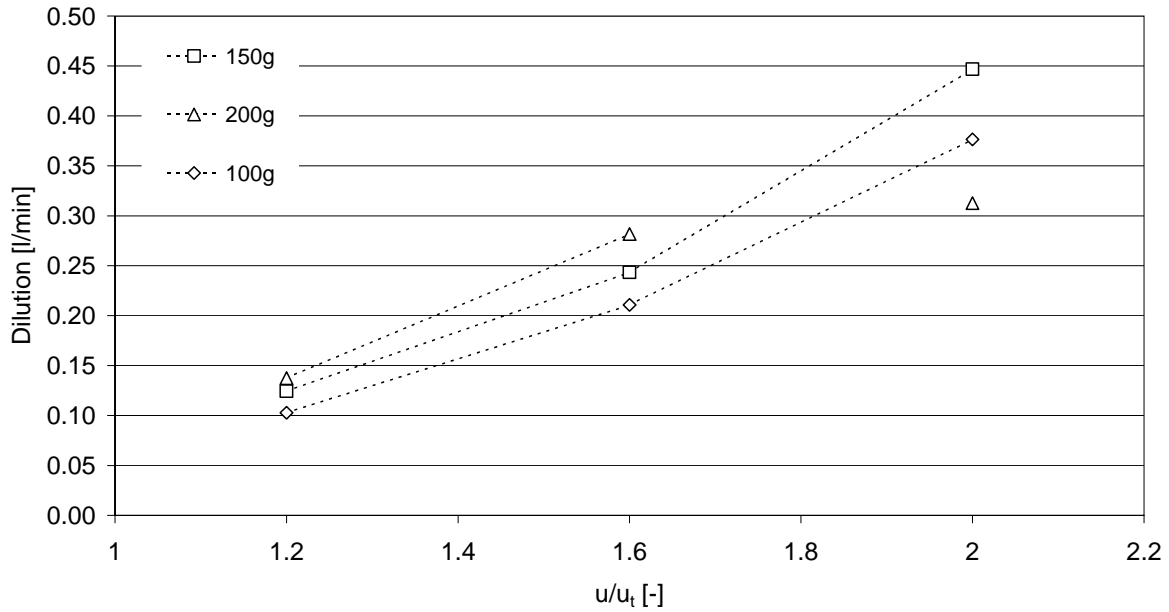
Figure 5-11: Absolute dilution into fuel reactor, slot height 5 mm, variation of V_{AR} , V_{FR} = 2.56 [l/min] = 20*u_{mf} [m/s]
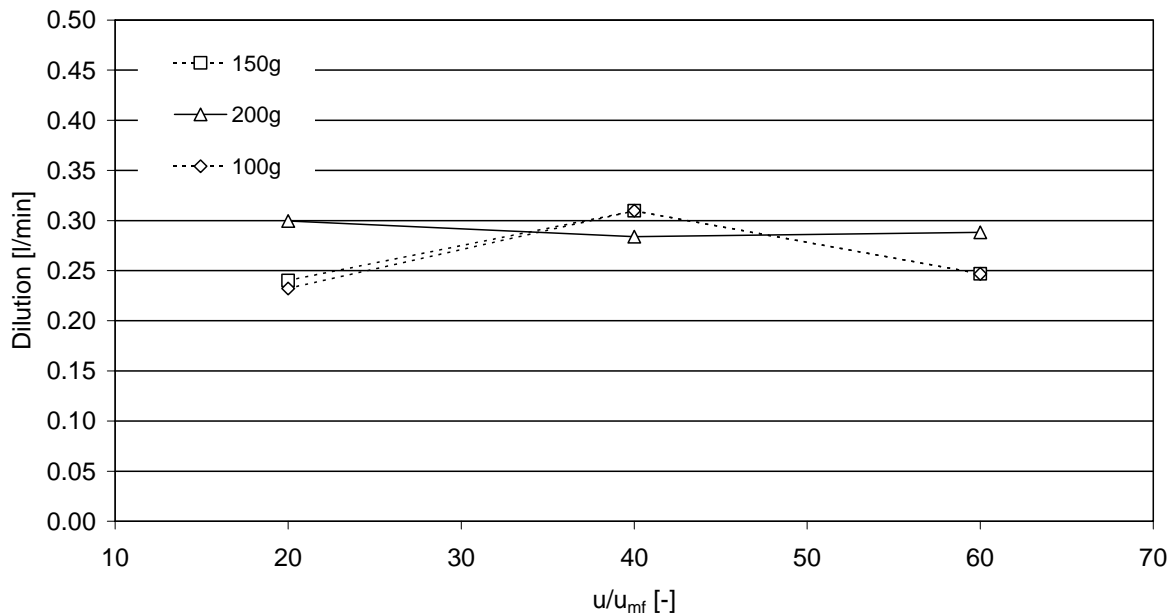

Figure 5-12: Dilution into fuel reactor, slot height 5 mm, variation of V_{FR} , V_{AR} = 31.32 [l/min] = 1.6*u_t [m/s]
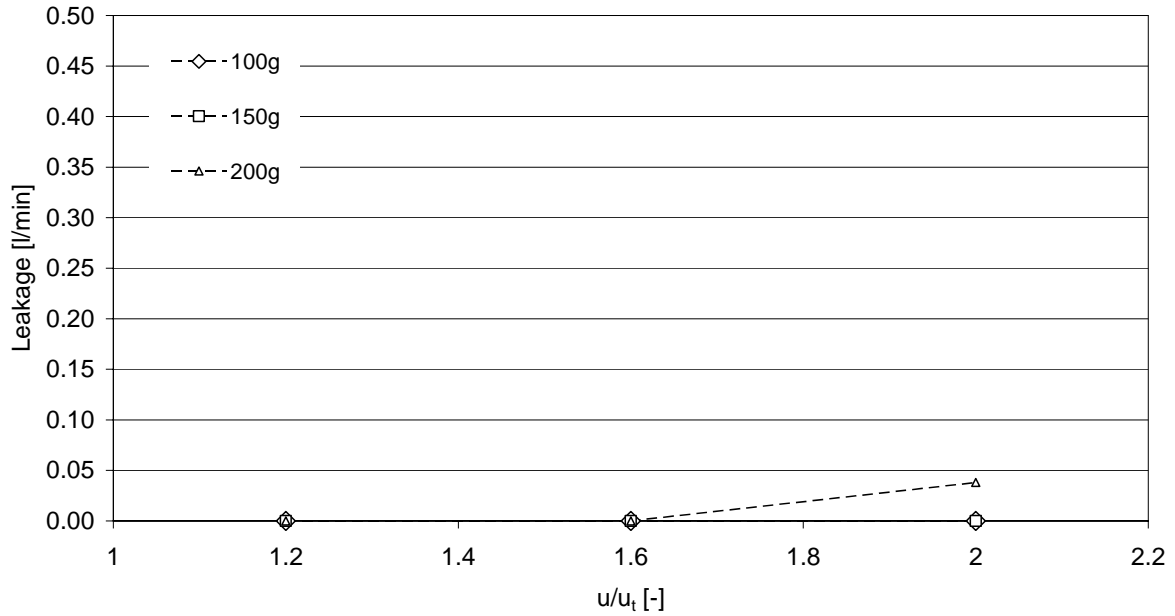
Slot Height 3.0mm:

Figure 5-13: Absolute leakage into air reactor, slot height 3 mm, variation of V_{AR}, V_{FR} = 2.56 [l/min] = 20*u_{mf} [m/s]
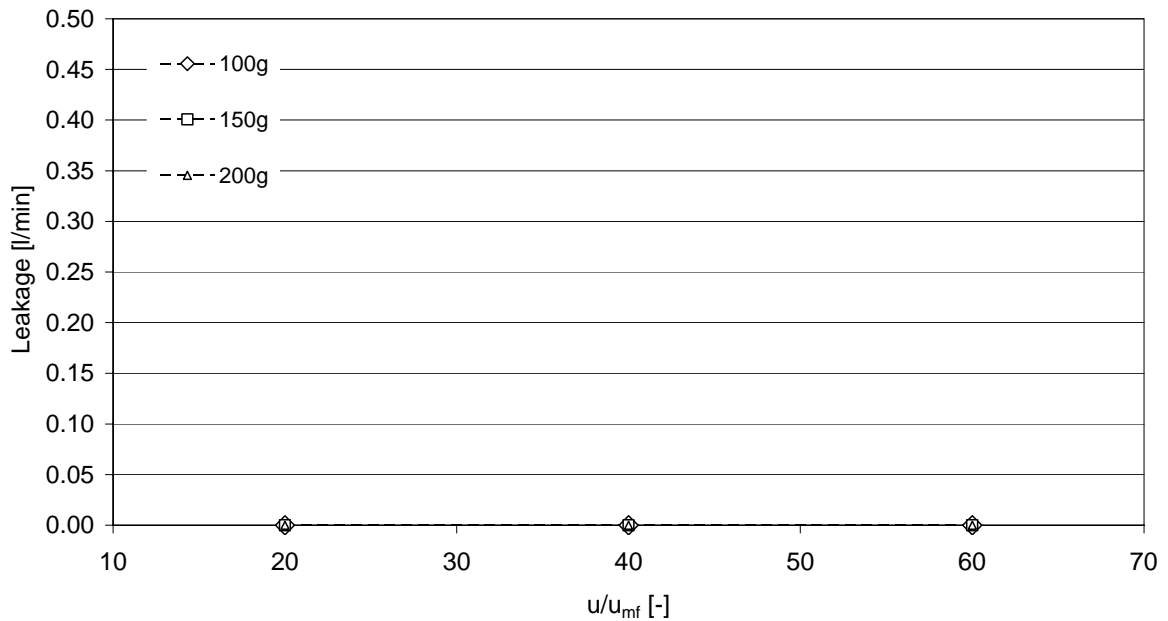

Figure 5-14: Absolute leakage into air reactor, slot height 3 mm, variation of V_{FR} , V_{AR} = 31.32 [l/min] = 1.6*u_t [m/s]
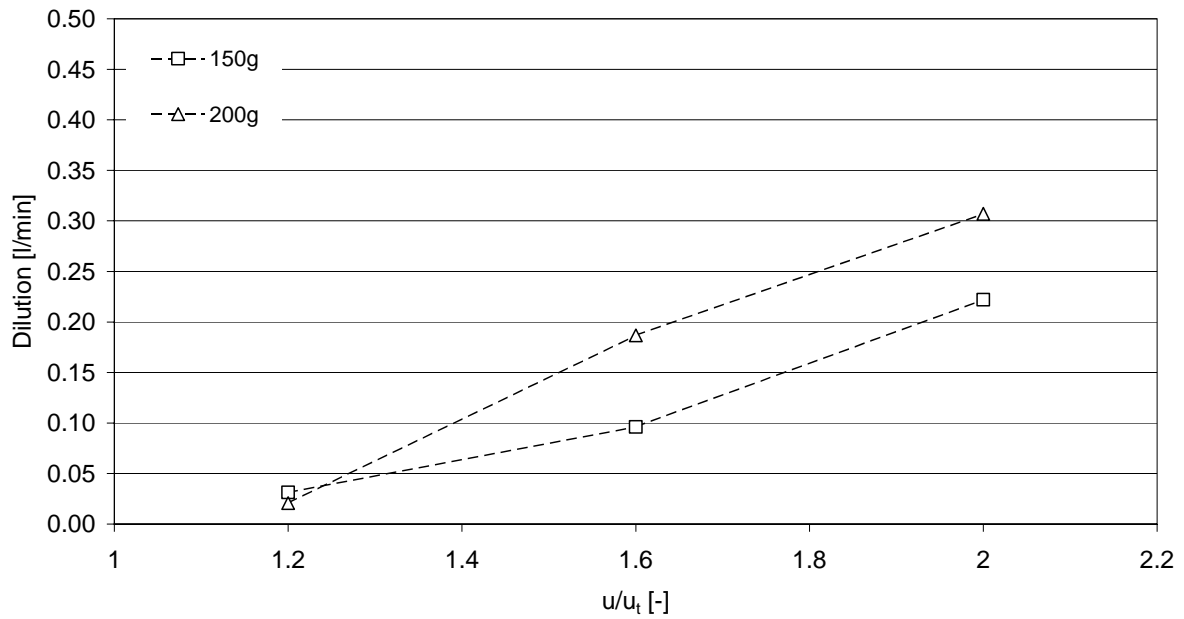
Figure 5-15: Absolute dilution into fuel reactor, slot height 3 mm, variation of V_{AR} , V_{FR} = 2.56 [l/min] = 20*u_{mf} [m/s]
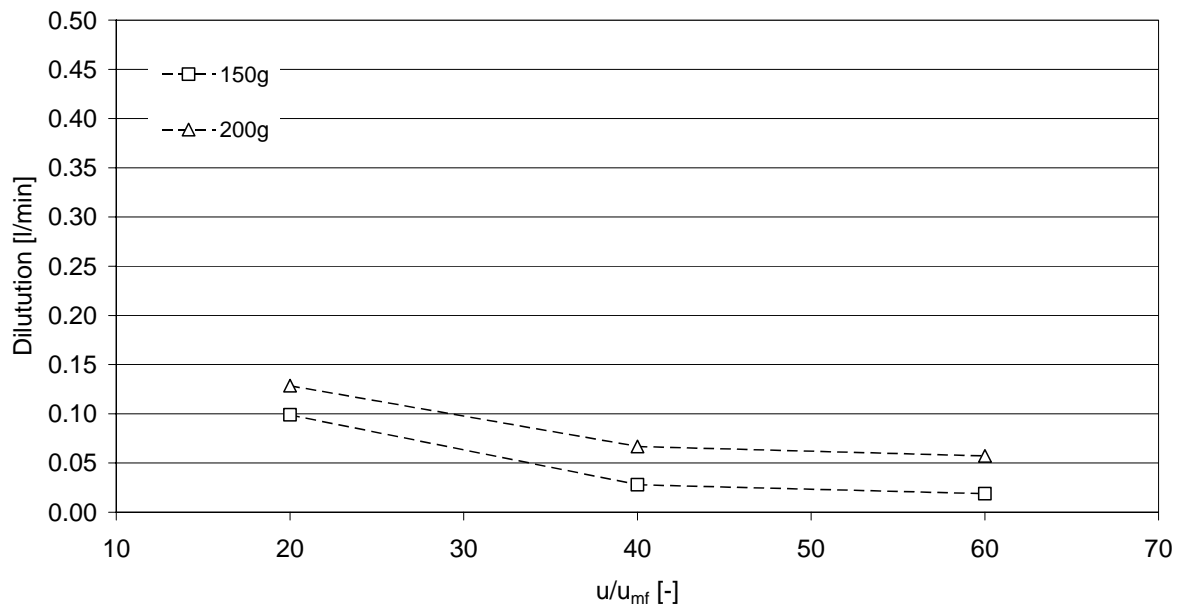

Figure 5-16: Absolute dilution into fuel reactor, slot height 3 mm, variation of V_{FR} , V_{AR} = 31.32 [l/min] = 1.6*u_t [m/s]
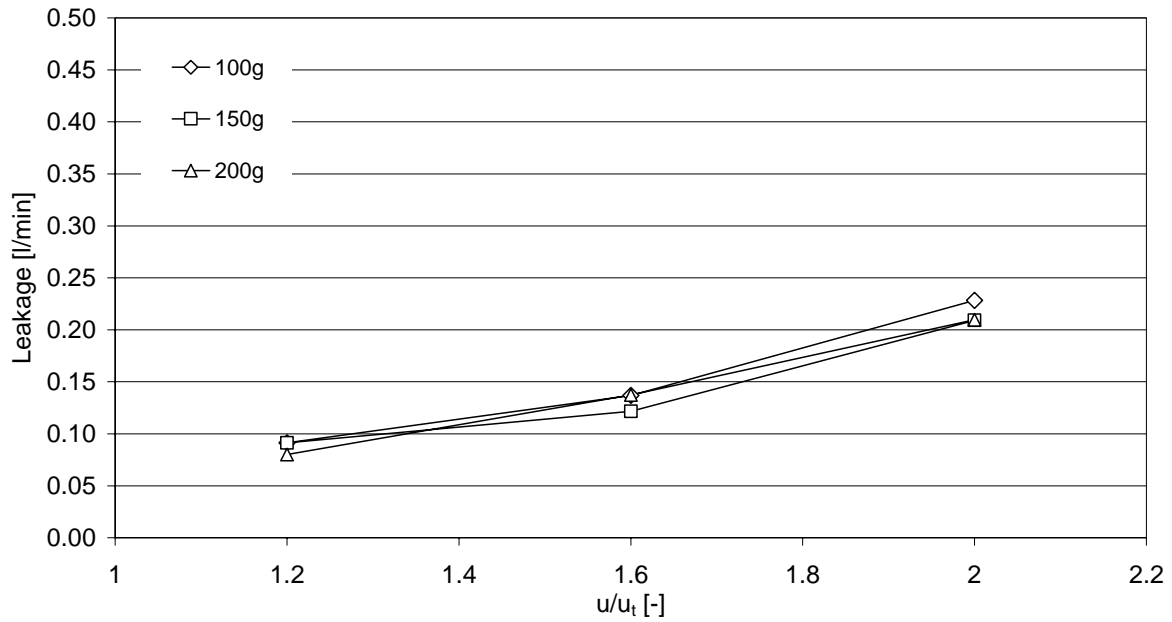
Slot Height 1.5mm:

Figure 5-17: Absolute leakage into air reactor, slot height 1.5 mm, variation of V_{AR}, V_{FR} = 2.56 [l/min] = 20*u_{mf} [m/s]

Figure 5-18: Absolute leakage into air reactor, slot height 1.5 mm, variation of V_{FR} , V_{AR} = 31.32 [l/min] = 1.6*u_{t} [m/s]

Figure 5-19: Absolute dilution into fuel reactor, slot height 1.5 mm, variation of V_{AR} , V_{FR} = 2.56 [l/min] = 20*u_{mf} [m/s]
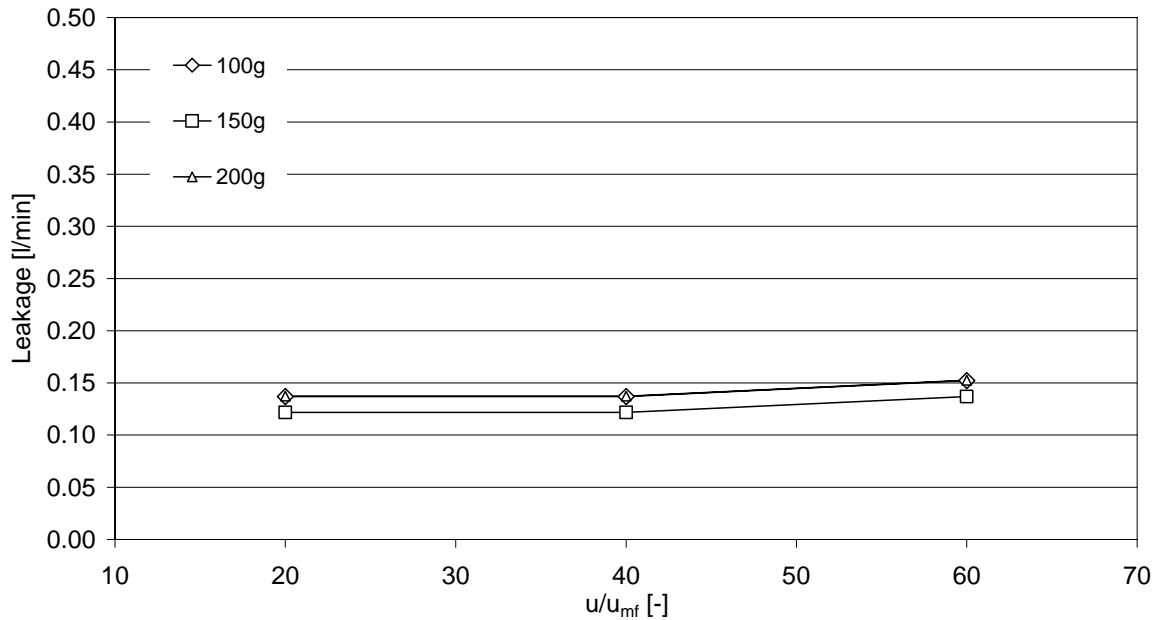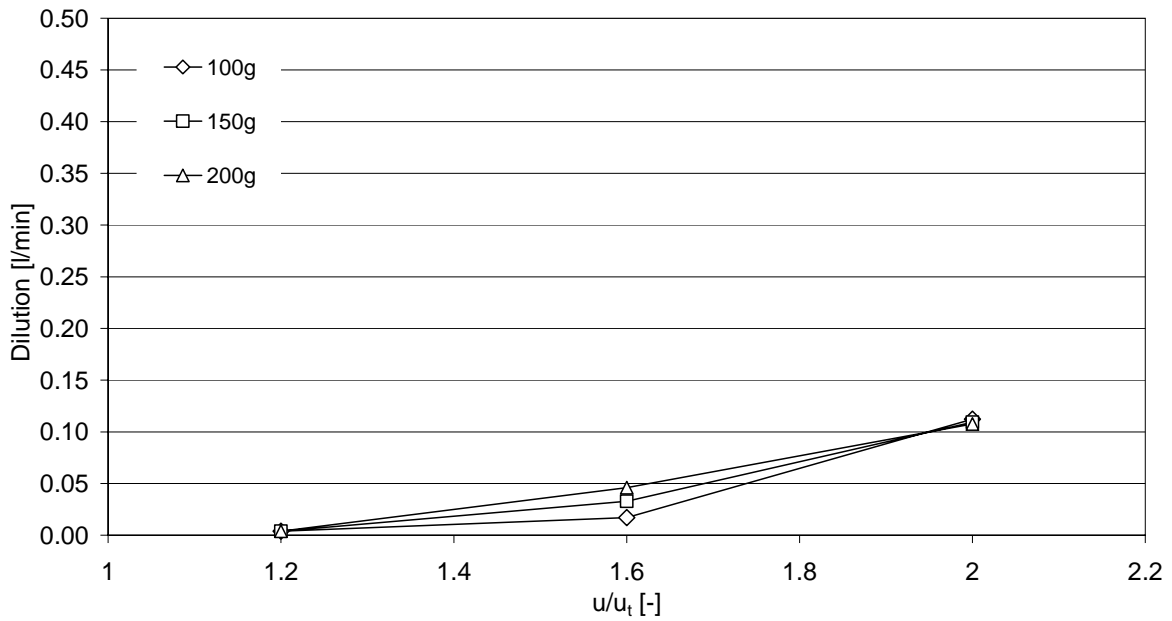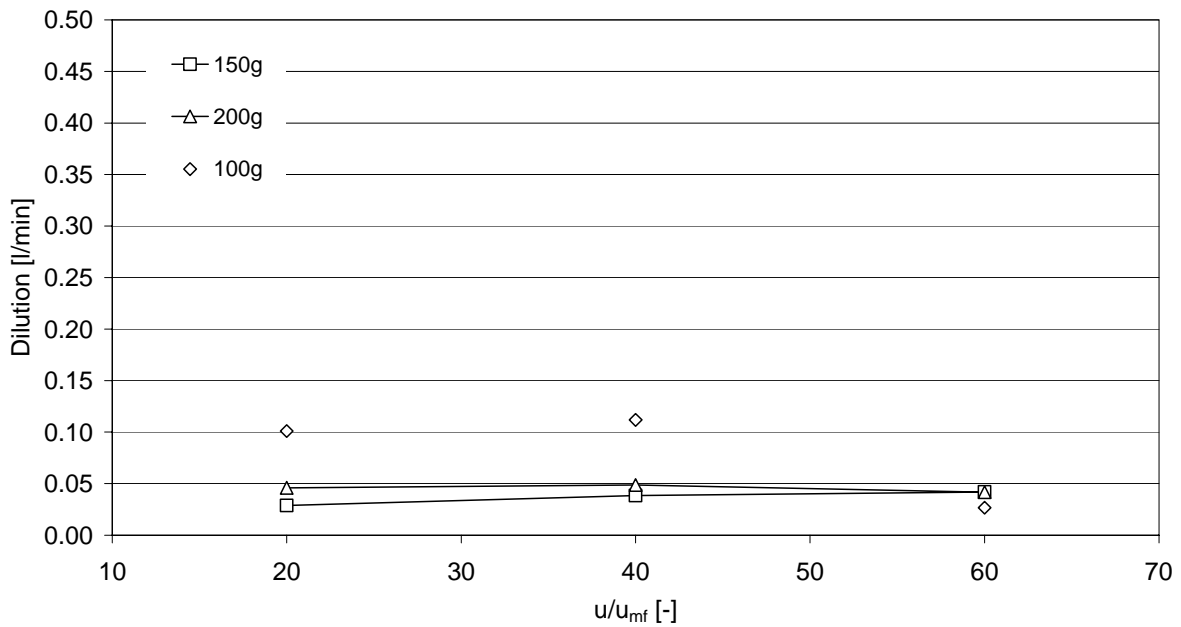

Figure 5-20: Absolute dilution into fuel reactor, slot height 1.5 mm, variation of V_{FR} , V_{AR} = 31.32 [l/min] = 1.6*u_t [m/s]

Figure 5-17 and Figure 5-19 show also very clearly that an increasing volume flow of the air reactor results in a higher amount of leakage and dilution. However, increasing the volume flow in the fuel reactor, did not affect the amount of leakage or dilution and the measured values remained nearly constant (Figure 5-18 and Figure 5-20) The conclusion is that the leakage and the dilution are strongly connected to the circulating solids, and therefore higher circulation forces higher gas transport through both of the orifices.

A closer look to Figure 5-20 raises the question, why the dilution with 100g solid inventory is significantly higher at lower fluidisation rates and then, at a higher fluidisation rate, obviously drops back to its expected value. An analysis of the contemporarily measured concentration of the analysis gas in the *air reactor* showed a drop in the concentration during lower fluidisation. This is a clear sign that in case of low solid inventory and low fluidisation on the fuel reactor side, bubbles even manage to slip through the 1.5 mm slot, as a result of the comparatively low pressure gradient between the reactors.

If the measured values of gas leakage and dilution for the experiment with the 1.5 mm slot are referred to the inlet gas stream of the equivalent reactor, a percental designation can be obtained. The leakage into the air reactor is the absolute leakage flow divided by the flow entering the fuel reactor and vice versa. Due to the higher fluidisation in the air reactor, the values for the dilution drop down to only 0.09 – 0.35%, whereas the values for the leakage are still relatively high at about 1.6 – 10.5%. Accordingly, the accuracy of the measured values for the leakage is lower than that for the dilution. The small amount of leakage gas that arrives in the air reactor is diluted approximately 10 to 15 times higher than in the fuel reactor and exact measurements are difficult to achieve. Therefore, a second set of measurements was taken for verification. The obtained values presented in Figure 5-21 and Figure 5-22 represent mean values.

Additionally, the measurements of the dilution are presented in a percental designation in Figure 5-23 and Figure 5-24 to demonstrate the comparably low values.

Figure 5-21: Percental leakage into air reactor, slot height 1.5 mm, variation of V_{AR}, V_{FR} = 2.56 [l/min] = 20*u_{mf} [m/s]

Figure 5-22: Percental leakage into air reactor, slot height 1.5 mm, variation of V_{FR}, V_{AR} = 31.32 [l/min] = 1.6*u_t [m/s]
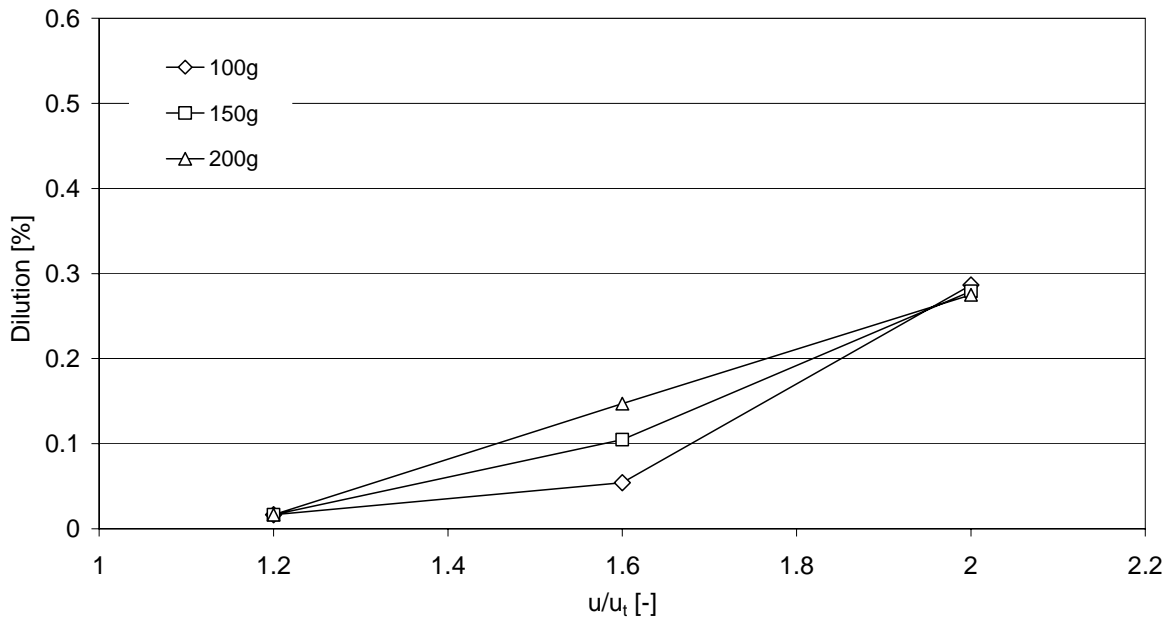
Figure 5-23: Percental dilution into fuel reactor, slot height 1.5 mm, variation of V_{AR}, V_{FR} = 2.56 [l/min] = 20*u_{mf} [m/s]
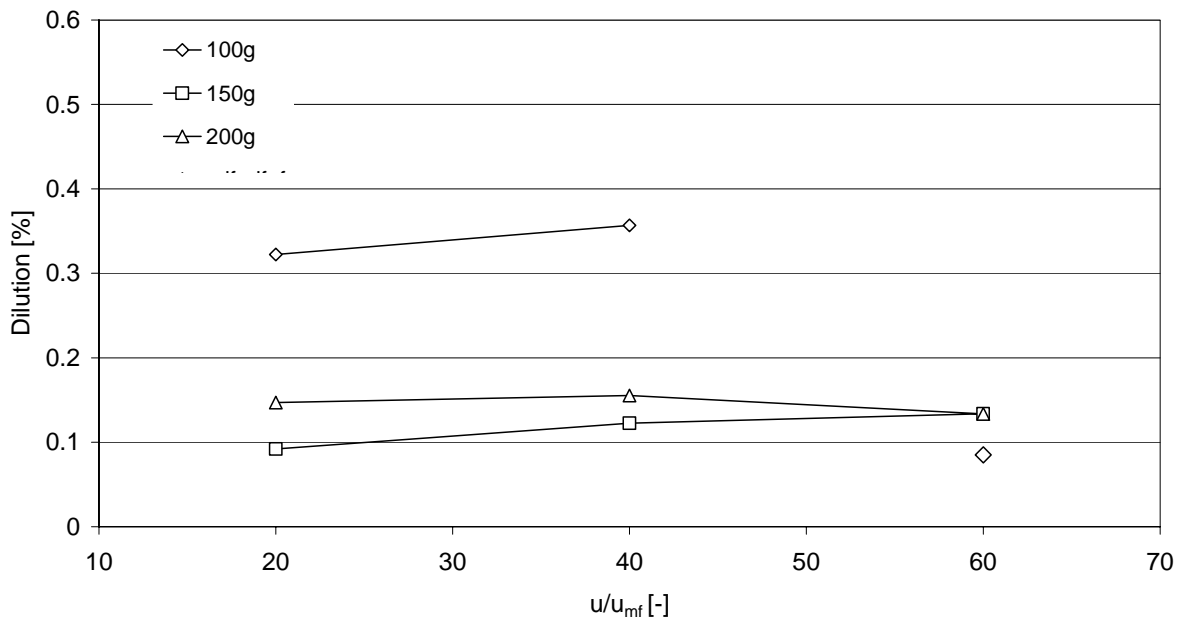
Figure 5-24: Percental dilution into fuel reactor, slot height 1.5 mm, variation of V_{FR}, V_{AR} = 31.32 [l/min] = 1.6*u_t [m/s]

Modification of the cold flow model

In the following the effects of the modifications on leakage and dilution are demonstrated. As already mentioned above, in was assumed that some of the gas leakage occurs when

bubbles slip thorough the slot due to local pressure differences between the two reactors. This effect was minimised by installing the higher slot boundary. In Figure 5-25 a clear reduction of the leakage values can be seen, attaining values between 0.5 and 4.5 per cent. Moreover the elongated downcomer section was attempted to enhance the effectiveness of a proper J-valve and reduce the dilution. The results are presented in Figure 5-26.
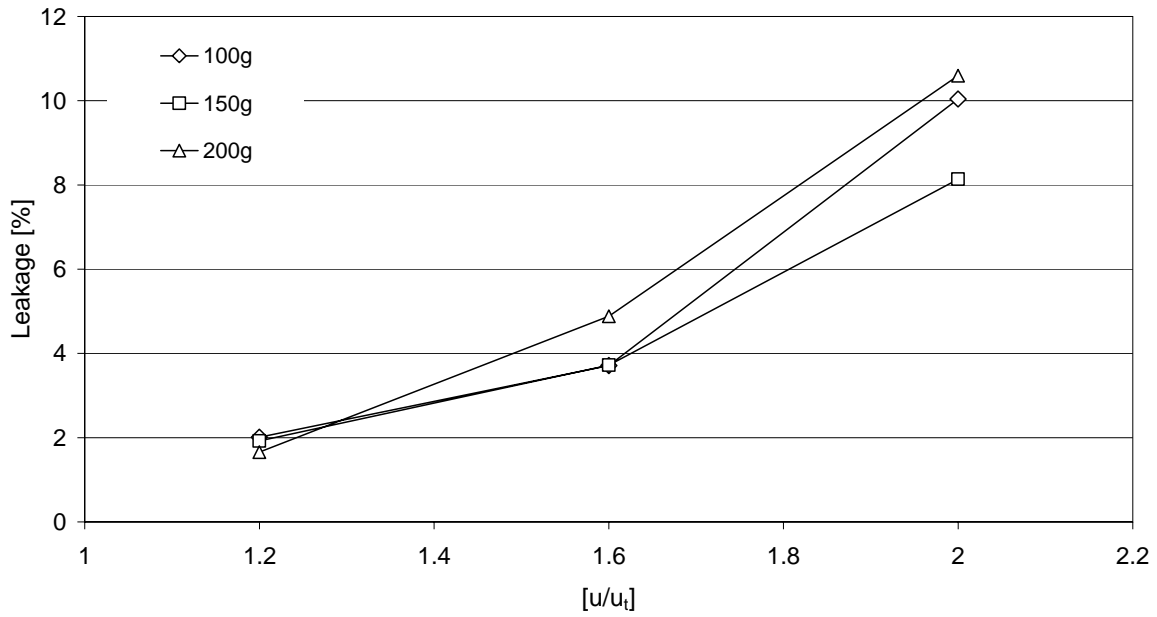

Figure 5-25: Comparison original/modified percental leakage into air reactor, slot height 1.5 mm, variation of V_{AR}, V_{FR} = 2.56 [l/min] = 20*u_{mf} [m/s]
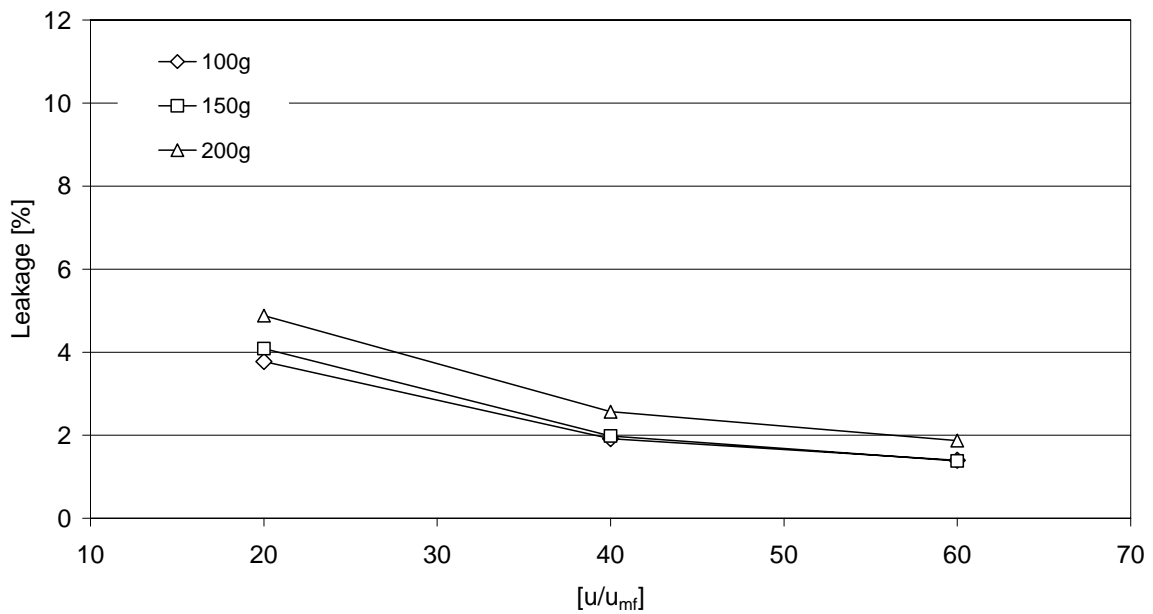

**Figure 5-26: Comparison original/modified percental dilution into fuel reactor, slot height 1.5 mm, variation of V_{AR}, V_{FR} = 2.56 [l/min] = 20*u_{mf} [m/s]**

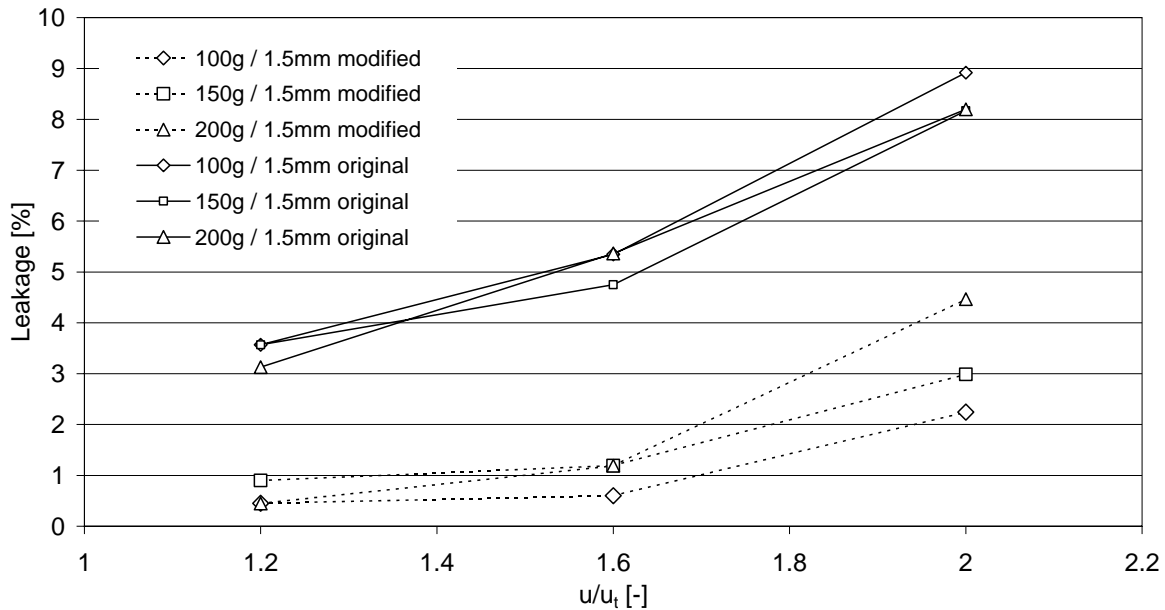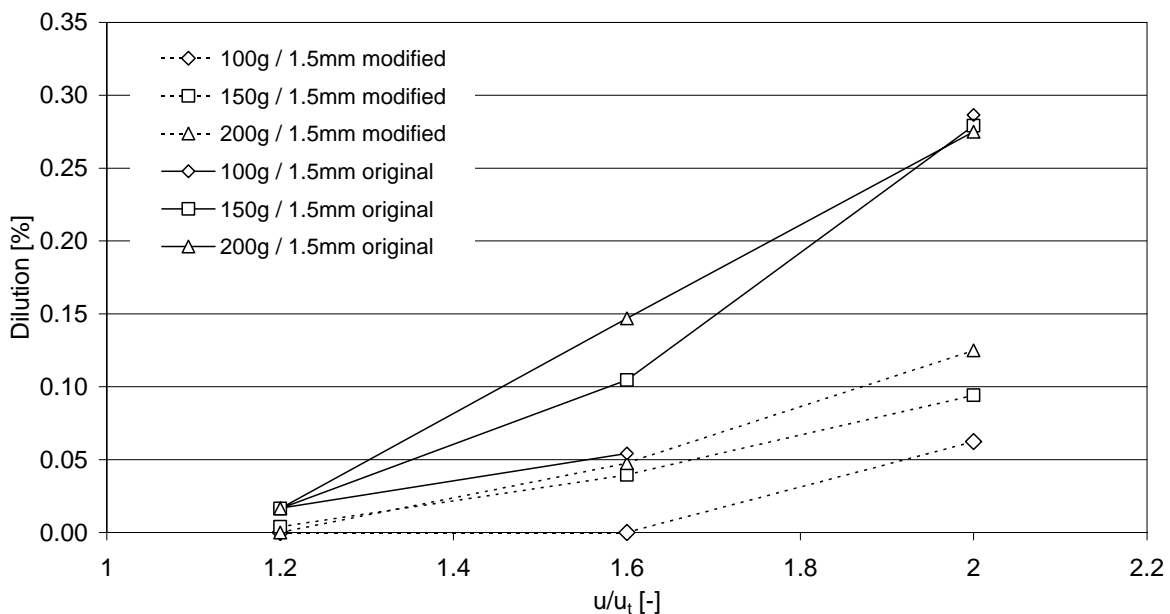### 5.4.3 Coherence between Gas Leakage and Solid Circulation Rate

In Figure 5-27 the absolute gas leakage is plotted against the solid circulation rate, to determine the coherence between those values. It can be seen that in the modified reactor the leakage increases linearly with the increasing solid circulation rate, and theoretically, no solid circulation means no gas leakage. Also the original reactor shows a linear increasing of the leakage but with a higher inclination and an intercept on the ordinate. Again, this can be interpreted as the part of leakage gas that slips through the orifice due to the local pressure differences.
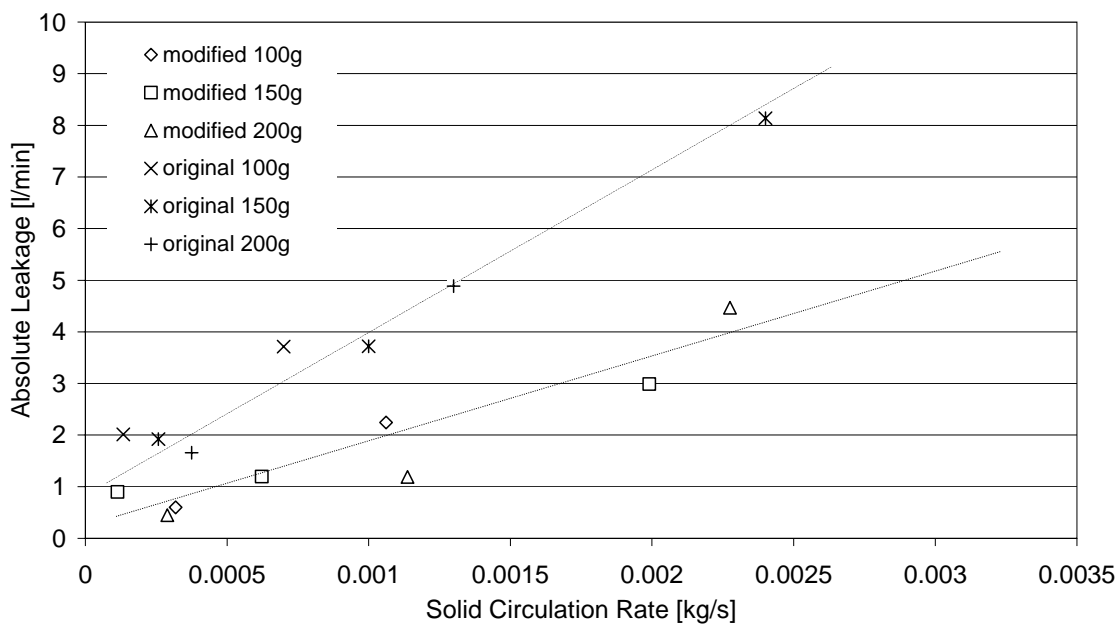
Figure 5-27: Coherence between solid circulation rate and leakage

Verification Measurements using Flame Ionisation Detection (FID)

In Chapter 5.2 an equal split of the fluidisation gases in the downcomer section and in the slot section was assumed. To verify this theory, methane was used as a tracer gas for the fluidisation of the slot section. The concentration of the gas was measured at the air reactor exit and at the fuel reactor exit and it was found that the major part of the tracer gas was detected in the air reactor. Virtually the same result was achieved in the measurements for the downcomer section. In the slot section, 78 – 99% of the fluidisation gas arrives in the air reactor, whereas in the downcomer section 84 – 99% arrives in the fuel reactor, depending on the amount of solid inventory introduced into the reactor and on the circulation rate of the system.

5.4.4 Pressure Profile

For the determination of the pressure profile over the reactor, the 6mm diameter pressure taps that were used for the measurements with the small scale cold flow model were replaced by injection needles with a diameter of 1.2mm. The advantage of this measure was that plugging could be avoided during most of the measurements.

Figure 5-28: Pressure profile over reactor height, solid inventory 150g, V_{AR} = 31.32 [l/min] = 1.6u_t, V_{FR} = 2.56 [l/min] = 20u_{mf}.
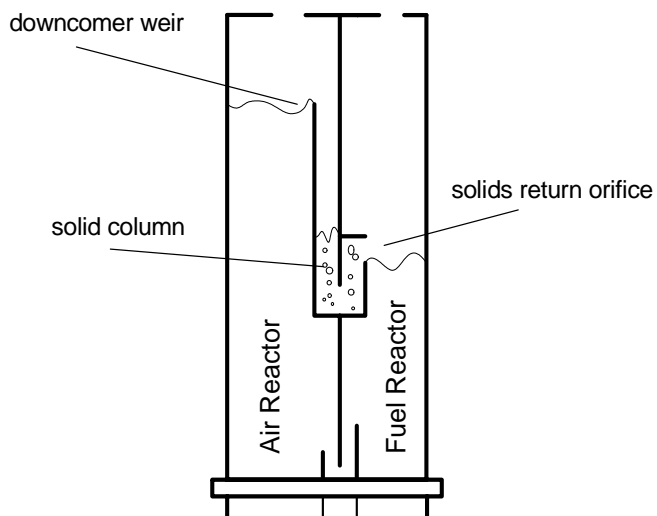
Figure 5-29: Height of downcomer weir and solids return orifice (schematic view)

For the values depicted in Figure 5-28, 150g of the powder were introduced into the reactor. It can be seen that the pressure difference of approximately 100Pa in the bottom area of the reactors is essential to maintain the circulation of the system. Accordingly, at the height of the solids return orifice (see Figure 5-29), a counter pressure of approximately 30Pa between FR and AR was measured. After introducing 200g of

the powder into the reactor, the counter pressure at the height of the solids return orifice in the downcomer decreases which is demonstrated in Figure 5-30. It can be assumed that the resulting pressure difference caused by particles that fall down into the chute remain the only driving force for the circulation. If more than 200g of solid inventory are introduced into the system, the counter pressure in this section could take negative influence in the circulation rate. A solid column in the downcomer would be formed, counterbalancing the pressure difference. The local height of the return orifice should be increased, to avoid the accumulation of the powder in the downcomer.
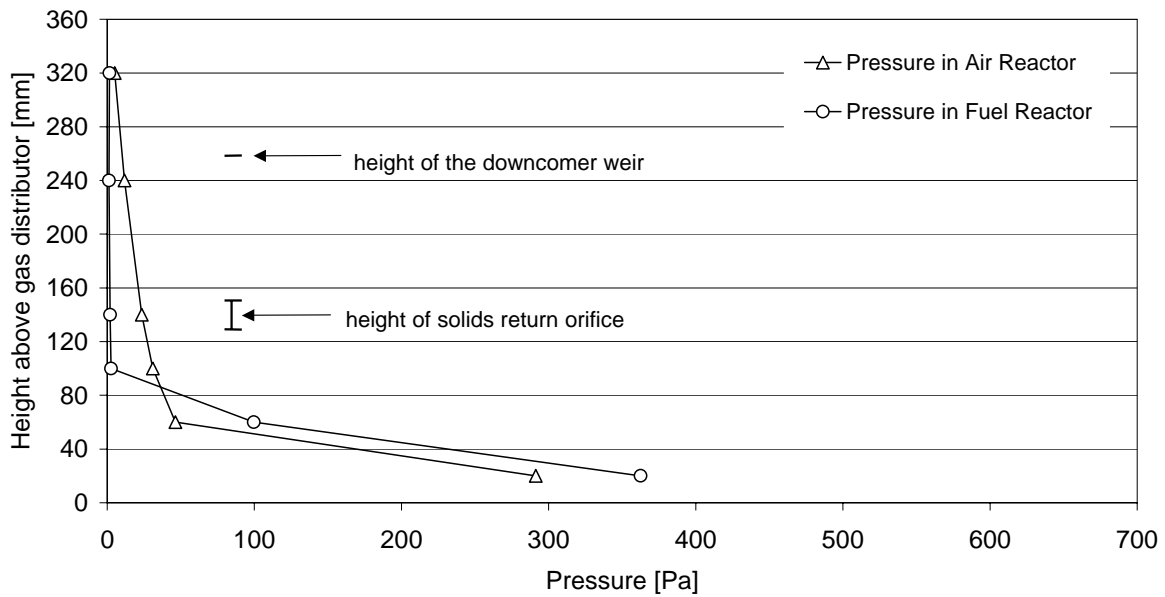

Figure 5-30: Pressure profile over reactor height, solid inventory 200g, V_{AR} = 31.32 [l/min] = 1.6u_t, V_{FR} = 2.56 [l/min] = 20u_{mf}
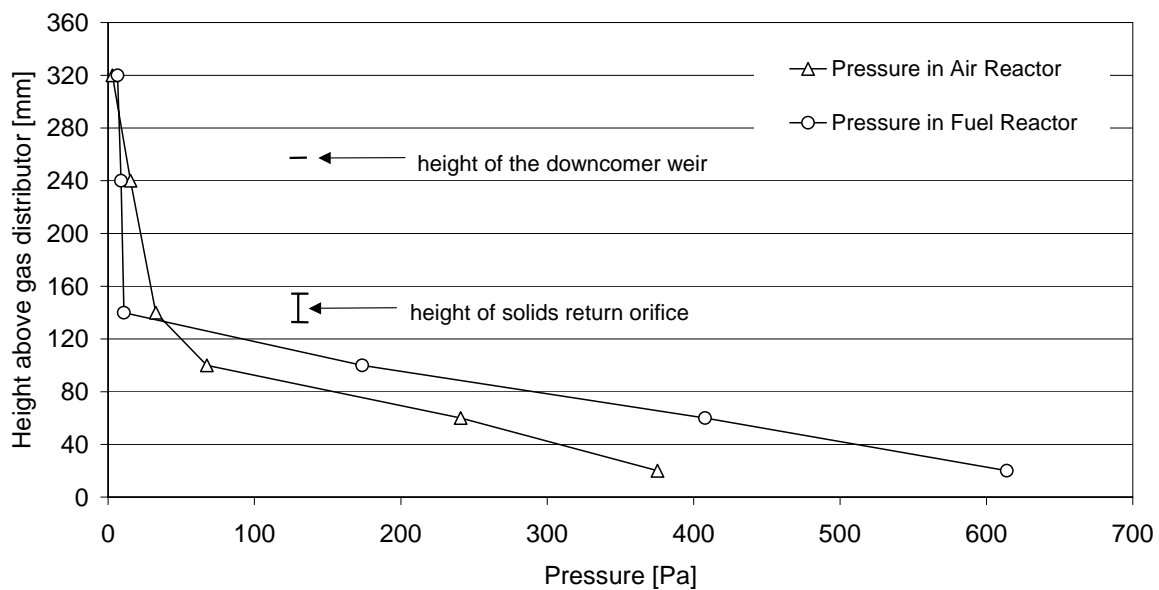
6 Recommendations for Design Modifications of the Hot Unit

In this chapter, a summary on the suggested design proposals based on the results of the previous section is given, which should be implemented into a "hot" laboratory unit. The hot reactor system is made of steel and is operated at a temperature of approximately 950°C and 800°C for CLC and CLR, respectively. An oxygen carrier is used instead of the FCC powder and inert gas is used for the fluidisation of the siphons. To reduce heat losses, the apparatus is fitted into an insulation box.

6.1 Transfer of the Attained Results

A direct transfer of the attained results from the presented mid scale cold flow model to the small 150mm "hot" reactor would have the advantage that the modified unit would fit into the existing insulation box. Also the modifications of the experimental setup for gas supply and concentration measurement could be kept simple. Due to the fact that the scaling criteria (here Glicksman, L.R. [1], see section 4.2) are not valid without the preliminary adoption of the gas and powder properties this transfer is difficult. The comparability of the results would not be given any more and additionally, the technical feasibility to craft the proposed measures at a small scale is doubtful.

Therefore a new "hot" reactor unit should be designed by applying the scaling laws of Glicksman on the length scale and fluidisation gas parameters of the mid scale cold flow model. The expected dimensions of the "hot" reactor unit are expected to be somewhat larger than the corresponding cold flow model, like it was calculated by Johansson, et al. [14].

Additionally, the following scale-independent recommendations for the modifications on the hot laboratory unit can be given:

1. The implementation of a J-type loop seal in the slot section by applying two additional walls that confine the slot section takes great influence in the reduction of the gas leakage. The walls should have a sufficient height (see Table 6-1), to avoid accidental gas exchange between the reactors through the 1.5mm slot.

cold flow model type	suggested wall heights [mm]
small scale	20
mid scale	40

Table 6-1: Suggested wall heights for slot area

2. Additional fluidisation in the slot section is necessary to maintain the circulation rate. A porous plate is not the best solution for the gas distribution because fluidisation right beneath the slot should be avoided The bubbles that emerge at this narrow section hinder the solid circulation rate. A pair of small tubes (or small holes) on both sides of the slot through which the fluidisation gas is led to the section is the better solution.

3. A wind box section consisting of three compartments is a good opportunity to realise the above mentioned proposals. Precise construction and crafting of this section is essential to avoid gas mixing between the compartments before the gas enters into the reactor.

4. If, implementing a u-shaped siphon, instead of the ramp at the end of the downcomer chute is technically not feasible, at least a step that holds the particle column should be considered (see Figure 4-1). Although this measure could not significantly lower the dilution values it is a good protection against the drainage of the downcomer and the resulting risk of dilution.

5. Also in the downcomer section, additional fluidisation is necessary to maintain the solid circulation rate. A small tube introduced through the reactor wall would be a sufficient measure.

6. The solid circulation rate can be increased significantly by implementing certain geometrical fixtures in the sloped part of the particle separator section. The powder would be collected and directly transported to the opening of the downcomer, avoiding the effect that the major part falls back into the bed. This measure represents also an easy way of controlling the solids circulation rate and the connected solids distribution between the reactors.

7 Outlook for Further Development of Small Scale CFB for CLC and CLR

As already discussed in the introduction of this thesis, a reduction of CO_2 in the atmosphere is only possible, if substantial measures will be realised quickly. The prospected rise in the world's energy consumption of 60 percent until 2030 exceeds the potential of renewable energy by far and so, fossil fuels are expected to account for almost 90% of the worldwide growth in energy demand [2]. At this point, Carbon Capture and Storage represents an interesting mid term strategy for the handling of the green house gas problem. It constitutes an alternative to renewable and nuclear energy sources and could also be a future possibility for countries to contribute to the reduction of CO_2 and to fulfil the Kyoto targets. An implementation of CCS into the legislative frame of the global CO_2 trading scheme would be an additional push for the future of this relatively new technology.

However, a lot of research needs to be done to be able to transform the existing concepts into an attractive option for heat and power generation. Regarding the future prospects and the further development of a small scale CFB in the form of an adjacent reactor system, it has to be admitted that the chances are presumably limited to laboratory scale applications. The before mentioned advantages like direct heat transfer through the reactor wall, short transport lines for the solids without moving parts and incomparable compactness are evident, but clearly, a direct geometrical scale-up to local heat generator, or an industrial scale local power plant with CO_2 capture is difficult. The existing engineering standards offer an entire palette of equipment for a variety of processes linked with a lot of experience for detail engineering of large CFBs. Even, as in this case, the process demands special features such as effective gas sealing, it would still be based on existing CFB technology.

From an economical point of view, the concept to design and investigate a reactor unit in a small scale to gain knowledge about critical parameters of the system is a very reasonable strategy. The investment costs for design and construction of a small apparatus as well as the operating expenses are marginal compared to a "retrofitting" of a large scale power plant. It should be possible to implement any small scale unit into an existing laboratory infrastructure which gives small science projects the chance to take part in the development of a well designed and optimised reactor concept.

From a technical point of view, it has to be admitted that a great number of solutions for the transformations of Chemical-Looping Technologies into large scale applications are still missing. Also, some of the existing concepts are still not sophisticated enough to be reliable outside the laboratory. Common problems that support this statement are for example:

The kinetics of the Cu-, Fe and Ni-based oxygen carriers are well known by now, but the test periods are limited to a time period of 300 hours and the total lifetime of the particles can only be estimated. Of course, any further investigations on the solid inventory can be conducted less costly, in a small apparatus.

This argument is also applicable for a further development of the Chemical-Looping Technology, like observing different operating conditions, alternating fuel compositions, the reactivity in a pressurised system, the affinity to form solid carbon in a Boudouard reaction or usage of solid fuels or even biomass.

Compared to other technologies, the efforts that have been undertaken to increase the efficiency of the processes, CLC and CLR are still in an early stage of development and probably multi compartment reactor systems are advantageous to attain different temperature levels for a better energy recovery. Also here, a preliminary cold flow modelling would be necessary.

Summed up, it can be said that the successful results of recent work on this topic form a basis for a future development. Further research work will reveal both, solutions and additional research subjects, for specific problems that need to be solved to be able to form CLC and CLR to competitive technologies. Therefore, it should be considered that modelling small scale CFB reactor systems is a good and effective solution to attain reliable and fast results.

8 Summary and Conclusions

Among several existing Carbon Capture and Storage (CCS) technologies, Chemical-Looping Combustion (CLC) and Chemical-Looping Reforming (CLR) are two new and promising technologies, capable to separate the greenhouse gas CO_2 at comparatively low costs and with low energy losses.

This study conveys the research work carried out for the further development of a compact laboratory scale CFB reactor system for CLC and CLR. The solid circulation rate and the gas leakage were investigated against variation of

- amount of solid inventory

- fluidisation rate of the air reactor

- fluidisation rate of the fuel reactor

Additionally, the effects of geometrical modifications of the downcomer and the slot section were studied and the measured values were compared with the original model.

Based on earlier investigations on an existing cold flow model with a reactor height of 150 mm, different design improvements with the predominating aim to reduce gas leakage between the two reactors were carried out. The reactor unit (a scale unit according to the fluid dynamic similarity criteria of Glicksman, L.R. [1]) is characterised by a downcomer section where the particles are transported over a weir due to the high fluidisation in the air reactor and then drop into a chute, where a solid column is formed. The column is held at its position due to a pressure difference between the two reactors.

The ramp at the end of the chute, which acts as a downcomer, in the original design, was changed into a step which represents an approach to a proper J-type loop seal. Additionally a small tube was introduced into the downcomer section to fluidise the standing particle column and maintain the circulation of the powder.

In the slot section, two additionally mounted barriers should prevent gas leakage caused by bubbles slipping through the 1.5mm slot, due to local pressure differences between air reactor and fuel reactor. Additional fluidisation was necessary also here, to maintain the circulation rate.

As expected, the solid circulation rate was directly connected to the fluidisation rate of the air reactor which was varied between 6.6 – 9.5 l/min corresponding to a terminal settling velocity of 1.4 to 2.0*u_t.

It was found that the solid circulation rate decreases due to the modifications from 0.25-0.9 g/s to a range of 0.16-0.55 g/s compared with the original model.

For the determination of the gas leakage between the air reactor and the fuel reactor a tracer-method was used. Via a mass-balance over the total system the split of the gas streams could be determined and it was observed that both, leakage and dilution are directly connected to the solid circulation rate. The measurements showed that the leakage from the fuel reactor to the air reactor could not be reduced significantly. In fact, the leakage was reduced from 12-15% to 8.5-14% by the modifications of the reactor, but with respect to the lower solid circulation rate no clear improvement could be obtained.

Interesting results could be attained regarding the leakage from the air reactor to the fuel reactor (dilution). It was found that the fluidisation rate of the fuel reactor has influence on the amount of solids in the fuel reactor, which furthermore took effect in the pressure balance of the system and consequently on the amount of gas leakage. At lower fluidisation rates around 20*u_{mf} the leakage was still high at approximately 4% but at fluidisation rates above 30*u_{mf} the leakage could be reduced significantly from 3.6% of the original design to 0.5% of the modified reactor.

Earlier investigations and findings in this study on the small scale cold flow model led to the conclusion that friction effects caused by the reactor walls have strong influence on the measurements as design improvements could not significantly lower the gas leakage between the reactors. As a consequence a larger reactor flow model was built and a more complex loop seal was implemented. The reactor height was increased to 300mm and a complex approach to a J-type loop seal was implemented in the downcomer section. The wind box section, with the additionally mounted barriers in the slot area was basically adopted in a larger scale from the small reactor unit.

Again it was found that the fluidisation velocity of the air reactor controls the circulation rate. The volume flow in the air reactor was varied between 23.49 and 39.15l/min, corresponding to a terminal settling velocity of 1.2 to 2.0*u_t. An influence of the fuel reactor fluidisation velocity could not be found at the comparatively high fluidisation velocities between 20 and 100*u_{mf}, corresponding to a volume flow of 2.56 to 12.8l/min. Furthermore, the amount of introduced solid inventory seemed to have a stronger effect on the circulation than a variation of the slot height. The solid circulation rate could be varied in a broad range between 0.0608

to 2.251 g/s, which corresponds to a specific solid circulation rate between 0.041 and 1.501 kg/sm^2, if the circulation rate is referred to the base area of the air reactor.

When investigating the gas leakage it was found that measurement results with a slot height of 5 and 3 mm were not satisfying because reasonable amounts of gas bubbles could slip accidentally into the other reactor causing very high leakage values from air reactor to the fuel reactor. Further decreasing the slot height to 1.5 mm could deliver more satisfying values for the gas leakage in a range of 3-9%.

After applying some geometrical modifications on the reactor unit, the leakage from the fuel reactor to the air reactor could be minimised to 0.5 – 4.5% at a fluidisation rate of 23.49 – 39.15 l/min corresponding to a velocity of 1.2 -2.0*u_t.

Accordingly, the gas leakage from the air reactor to the fuel reactor could be minimised to a range of 0.02 – 0.13%.

The findings of the experiments show the general suitability of the concepts for the planned applications. The design recommendations for the adaptation of the hot unit for CLR operation can be summed up as follows:

- Implementation of a J-type loop seal in the slot section by applying two additional walls that confine the slot section.

- Additional fluidisation in the slot section is necessary to maintain the circulation rate.

- A wind box section consisting of three compartments is a good opportunity to realise the above mentioned proposals.

- If, implementing a u-shaped siphon, instead of the ramp at the end of the downcomer chute is technically not feasible, at least a step that holds the particle column should be considered.

- Also in the downcomer section, additional fluidisation is necessary to maintain the solid circulation rate. A small tube introduced through the reactor wall would be a sufficient measure.

- The solid circulation rate can be increased significantly by implementing a ramp in the particle separator section that transports the powder directly to the opening of the downcomer.

9 Nomenclature

Symbols

A_{Slot}	area of slot	$[m^2]$
$c_{AR,I}$	concentration at air reactor inlet	[l/l]
$c_{AR,E}$	concentration at air reactor exit	[l/l]
c_{DO}	concentration at downcomer fluidisation inlet	[l/l]
$c_{FR,I}$	concentration at fuel reactor inlet	[l/l]
$c_{FR,E}$	concentration at fuel reactor exit	[l/l]
c_{SL}	concentration at slot fluidisation inlet	[l/l]
D	Diameter	[m]
d_p	particle diameter	[m]
F_S	specific solid circulation rate (referred to A_{Slot})	$[kg/sm^2]$
Fr	Froude number	[-]
G_S	specific solid circulation rate	$[kg/sm^2]$
ΔH_C	enthalpy from combustion	[kJ/mol]
ΔH_{ox}	enthalpy from oxidation	[kJ/mol]
ΔH_{red}	enthalpy from reduction	[kJ/mol]
L	length	[m]
Re_P	particle Reynolds number	[-]
u_{mf}	minimum fluidisation velocity	[m/s]
u_t	terminal velocity	[m/s]
V_{AR}	volume flow of air reactor	[l/min]
V_{FR}	volume flow of fuel reactor	[l/min]
$\dot{V}_{AR,I}$	inlet volume flow of air reactor	[l/min]
$\dot{V}_{AR,E}$	exit volume flow of air reactor	[l/min]
$\dot{V}_{DO}$	inlet volume flow of downcomer section	[l/min]
$\dot{V}_{FR,I}$	inlet volume flow of fuel reactor	[l/min]
$\dot{V}_{FR,E}$	exit volume flow of fuel reactor	[l/min]

$\dot{V}_{SL}$	inlet volume flow of slot section	[l/min]

Greek letters

ε	void fraction	[-]
ϕ	particle sphericity	[-]
ρ_p	particle density	[kg/m^3]

Acronyms

AR	Air Reactor
CCS	Carbon Capture and Storage
CFB	Circulating Fluidised Bed
CLC	Chemical Looping Combustion
CLR	Chemical Looping Reforming
CSS	CO2 Separierung und -Speicherung
EOR	Enhanced Oil Recovery
EGR	Enhanced Gas Recovery
FCC	Fluid Catalytic Cracking
FID	Flame Ionisation Detector
FR	Fuel Reactor
GS	Geological Storage
MFC	Mass Flow Controller
PSD	Particle size distribution
TSI	Total Solid Inventory
ZET	Zero Emission Technologies

10 References

[1] Glicksman, L.R., Scaling relationships for fluidized beds, Chem. Eng. Sci. 39 (9), 1373-1379 (1984).

[2] Pflüger, A., "An Energy and Technology Roadmap", VGB PowerTech, Volume86, p. 30-33 (2006).

[3] Worldwide Report, Oil & Gas Journal (2005).

[4] DIRECTIVE OF THE EUROPEAN PARLIAMENT AND OF THE COUNCIL of 13 October 2003 establishing a scheme for greenhouse gas emission allowan*ce trading within the Community and amending Council Directive 96/61/EC (2003).*

[5] IEA Energy Technology Scenarios Series, Prospects for CO_2 Capture and Storage (CCS), Review draft (October 2004).

[6] Papay, J., Synergy of Petroleum Recovery Methods, Erdöl Erdgas Kohle, Heft 9 121. Jahrgang (September 2005).

[7] Wilson M., Monea M., IEA GHG Weyburn CO_2 monitoring and storage project summary report 2000-2004, From the proceedings of the 7th international conference on greenhouse gas control technologies, 5-9 Sep 2004, Vancouver, Canada, 273 pp (2004).

[8] Gielen D., Podkanski J., IEA, Energy 3/2004 (2004).

[9] Salvador, C., Lu, D., Anthony, E. J., Abanades, J. C., Novel CO_2 control method by means of CO_2 chemical looping, 7th International Conference on Energy for a Clean Environment, 7-10 July, Lisbon (2003).

[10] Richter H.J., Knoche K.F., Reversibility of combustion processes, ACS Symposium Series, Washington DC, 235; p. 71-85 (1983).

[11] Anheden, M. and Svedberg, G., Exergy analysis of chemical-looping combustion systems, Energy Conversion Management, 39, 16-18, 1967-1980 (1998).

[12] Rydén M., Hydrogen production with carbon dioxide capture by reforming of natural gas using chemical-looping technologies, PhD Thesis, Chalmers University of Technology, Sweden, 2006.

[13] Kronberger, B., Johansson, E., Löffler, G., Mattisson, T., Lyngfelt, A., Hofbauer, H., A two-compartment fluidized bed reactor for CO_2 capture by chemical-looping combustion, Chem. Eng. Technol., 27, No.12, p. 1318-1326 (2004).

[14] Johansson, E., Mattisson, T., Lyngfelt, A., Thunman, H., A 300 W laboratory reactor system for chemical-looping combustion with particle circulation, Fuel, Volume 85, Issues 10-11, p. 1428-1438 (2006).

[15] Chong, Y.–O., Nicklin D.J., Tait P. J., Solids exchange between adjacent fluid beds without gas mixing, Powder Technology, 47 (1986) 151 – 156.

[16] Reichhold, A., Hofbauer, H., Internally circulating fluidized bed for continuous adsorption and desorption, Chemical Engineering and Processing, 34 (1995) 521 – 527.

[17] Fang, M., Yu, C., Shi, Z., Wang, Q., Luo, Z., Cen, K., Experimental research on solid circulation in a twin fluidized bed system, Chemical Engineering Journal, 94 (2003) 171 – 178.

[18] Snieders, F.F., Hoffmann, A.C., Cheesman, D., Yates, J.G., Stein, M., Seville, J.P.K., The dynamics of large particles in a four-compartment interconnected fluidized bed, Powder Technology, 101 (1999) 229 – 239.

[19] Korbee, R., Regenerative desulfurisation in an interconnected fluidised bed system, PhD thesis, Delft University of Technology, Netherlands, 1995.

[20] O.C. Snip, The interconnected fluidized bed reactor for gas/solids regenerative process, PhD Thesis, Delft University of Technology, Netherlands, 1997.

[21] B.M. Wagenaar, W. Prins, W.P.M. Van Swaaij, Pyrolysis of biomass in the rotating cone reactor: modelling and experimental justification, Chem. Eng. Sci. 49 5109-5126 (1994).

[22] A.M.C. Janse, P.Maarten Biesheuvel, Wolter Prins, Wim P.M. van Swaaij, A novel interconnected fluidised bed for the combined flash pyrolysis of biomass and combustion of char, Chem. Eng. Jour. 76 (200) 77-86 (1999).

[23] Li, X. G., Liu D.L., Kwauk, M.S., Proc. Joint Meeting of Chem. Eng., SIESC and AIChE, Chem. Industry Press, Beijing, 1982, pp. 382 – 391.

[24] Liu, D. L., Li, X. G., Kwauk M.S., in J.R. Grace and J.M. Matsen (eds.), Fluidization, Plenum, New York, 1980, pp. 485 – 492.

[25] Leung, L.S., Chong,Y.O., Lottes, J., Operation of V Valves for Gas-Solid Flow, Powder Technology 49 (1987) 271-276.

[26] Guigon, P.,Yuan, M., Large, J.F., Vernotte, V., Controlled internal circulating fluidized bed heat exchanger, Proceedings of the Third International Conference on Circulating Fluidized Beds, Nagoya, Japan, 1990, pp 289 – 294.

[27] B. Bhattacharya, D. Sathiyamoorthy, V. Govardhana Rao, S.P. Mahajan, Solid circulation in a compartmented gas fluidized bed, Powder Technology 101 (1999) 191-204.

[28] Hofbauer, H., Experimentelle Untersuchungen an einer zirkulierenden Wirbelschicht mit Zentralrohr, PhD thesis, Vienna University of Technology, (1982).

[29] Song, B.H., Kim, Y.T., Kim, S.D., Circulation of solids and gas bypassing in an internally circulating fluidized bed with a draft tube, Chem. Eng. Jour. 68 (1997) 115 - 122.

[30] Reichhold, A., Entwicklung von Reaktions/Regenerationssystemen für Adsorptions/Desorptionsprozesse und für katalytisches Cracken auf Basis von intern zirkulierenden Wirbelschichten, PhD thesis, Vienna University of Technology (1996).

[31] Chandel, M.K., Alappat, B.J., Pressure drop and gas bypassing in recirculating fluidized beds, Chem. Eng. Sci. 61 (2006) 1489 – 1499.

[32] Jeon, J.H., Kim, S.D., Kim, S.J., Kang, Y., Hydrodynamic Characteristics of binary solids mixtures in a square internally circulating fluidized bed, Proceedings of the 19th FBC Conference, Vienna, Austria, 2006.

[33] Chen, T.Y., Walawender, W.P., Fan, L.T., Transfer of Solids between Parallel Fluidised Beds, AIChE Symposium Series, 176, Volume 74, pp 75 - 81, (1978).

[34] Fercher, E., Experimentelle Untersuchungen an extern zirkulierenden Wirbelschichten, Master Thesis, Vienna University of Technology, (1983).

[35] Tagwerker, C., Aufbau und Betrieb eines Labormodells zur Untersuchung der Fluiddynamik eines Chemical Looping Combustion Wirbelschicht Systems, Master Thesis, Vienna University of Technology, 2003.